NASA TECHNICAL NOTE

NASA TN D-3929

NASA TN D-3929

MEASUREMENT OF PERFORMANCE, INLET FLOW CHARACTERISTICS, AND RADIATED NOISE FOR A TURBOJET ENGINE HAVING CHOKED INLET FLOW

by Jimmy M. Cawthorn, Garland J. Morris, and Clyde Hayes

Langley Research Center
Langley Station, Hampton, Va.

NATIONAL AERONAUTICS AND SPACE ADMINISTRATION • WASHINGTON, D. C. • MAY 1967

NASA TN D-3929

MEASUREMENT OF PERFORMANCE, INLET FLOW CHARACTERISTICS, AND RADIATED NOISE FOR A TURBOJET ENGINE HAVING CHOKED INLET FLOW

By Jimmy M. Cawthorn, Garland J. Morris, and Clyde Hayes

Langley Research Center
Langley Station, Hampton, Va.

NATIONAL AERONAUTICS AND SPACE ADMINISTRATION

For sale by the Clearinghouse for Federal Scientific and Technical Information
Springfield, Virginia 22151 – CFSTI price $3.00

MEASUREMENT OF PERFORMANCE, INLET FLOW CHARACTERISTICS, AND RADIATED NOISE FOR A TURBOJET ENGINE HAVING CHOKED INLET FLOW

By Jimmy M. Cawthorn, Garland J. Morris,
and Clyde Hayes
Langley Research Center

SUMMARY

A static test has been conducted to evaluate the effects of a choked inlet on the inlet performance, engine performance, and noise produced by a turbojet engine. Engine and inlet performance and sound measurements were made during tests with a small turbojet engine equipped with a three-dimensional, variable-geometry supersonic inlet. Tests were made for a range of inlet areas obtained by translating the inlet centerbody.

No increase in engine vibration was observed with the inlet choked and no erratic engine behavior was noted when the inlet was rapidly unchoked. For each centerbody position some engine performance losses were incurred at the lowest speed at which the inlet choked. The losses increased rapidly as engine speed was increased above the choking speed for each centerbody location and the rapid increase in exhaust gas temperature to the maximum allowable value prevented further increases in engine speed over the normal operational range.

Choking occurred at a value of total-pressure ratio of approximately 0.93 for the range of centerbody positions at which the inlet could be choked. Total-pressure loss and low velocities near the outer duct wall were found to result from the sharp leading edge with the centerbody located near the design position. Moving the centerbody forward so that the inlet minimum was located near the leading edge caused the losses to become increasingly large.

Noise measurements indicated that choking the inlet flow was beneficial in reducing the noise levels forward of the engine. Noise reductions of 2 to 5 dB were observed in the overall noise levels and 2 to 20 dB were observed in the noise levels of the fundamental-blade-passage frequencies.

INTRODUCTION

Aircraft noise in the vicinity of airports has imposed a severe operational problem, particularly for the case of landing approach during which the engines are operating at a reduced power setting and the objectionable discrete-frequency high-pitched compressor noises are predominant.

A possible method of reducing compressor noise heard on the ground in front of the airplane during an approach is to choke the inlet and thus create a small region of supersonic flow. Theoretically, the sound cannot propagate through this choked flow region and thus cannot exit from the mouth of the inlet. The benefits of inlet choking with regard to noise reduction have been demonstrated on full-scale turbojet engines with sonic plug devices. (See refs. 1 and 2.)

The objectives of the studies of this paper were to determine the effects of inlet choking on the noise radiated from the compressor of an axial-flow turbojet engine along with the associated engine and inlet performance. The tests were conducted with a small turbojet engine equipped with a three-dimensional variable-geometry supersonic inlet.

Engine and inlet performance and sound measurements were made during the tests for a range of engine speeds and inlet operating conditions, and the combined results are presented herein.

SYMBOLS

A	duct cross-sectional area, square feet (meters^2)
A_c	inlet capture area, square feet (meters^2)
F_n	engine net thrust, lb (newtons)
M	Mach number
N	engine rotational speed, rpm
N_{std}	rated maximum take-off engine rotational speed, 13 800 rpm
p_a	atmospheric pressure, pounds/square foot (newtons/meter^2)
p_t	total pressure, pounds/square foot (newtons/meter^2)

$\overline{p_t}$ average total pressure, pounds/square foot (newtons/meter^2)

r distance outward from inlet center line, inches (centimeters)

r_b radius of blunt-leading-edge external contour, inches (centimeters)

r_c centerbody radius, inches (centimeters)

r_d duct internal radius, inches (centimeters)

T_e engine exhaust gas temperature, ^oC (^oK)

W_f engine fuel flow, lbm/hr (kilograms/hour)

x axial distance, measured positive downstream from centerbody apex with centerbody at design position, inches (centimeters)

Δx longitudinal displacement of centerbody from design position (positive values indicate that centerbody is forward of design position), inches (centimeters)

δ ratio of total pressure to NASA standard sea-level pressure of 2116 lb/sq ft (101 314 newtons/meter^2)

θ ratio of total temperature to NASA standard sea-level temperature of 518.7^o R

ϕ rake position, positive clockwise facing upstream from top center, deg

Engine performance parameters for standard sea-level conditions:

$\frac{F_n}{\delta}$ corrected engine trust, lbf (newtons)

$\frac{N}{N_{std}\sqrt{\theta}}$ corrected engine speed, percent rated rpm

$\frac{T_e}{\theta}$ corrected exhaust temperature, ^oC

$\frac{W_f}{\delta\sqrt{\theta}}$ corrected fuel flow, lbm/hr (kilogram/hour)

$\frac{W_f}{F_n\sqrt{\theta}}$ corrected thrust specific fuel consumption

APPARATUS AND METHODS

Description of Engine and Installation

A Viper 8 jet turbine engine which was used for the investigation is shown in the photograph of figure 1. The engine incorporated a seven-stage axial-flow compressor driven by a single-stage axial-flow turbine. With fuel having a specific gravity of 0.80, the engine is rated for maximum take-off and operational necessity (10-minute limit) at 1750 pounds (7784 newtons) thrust at 13 800 rpm with an air mass flow of 32 pounds per second (142.34 newtons) for standard sea-level conditions.

The engine fuel system includes a fuel pump, a barometric flow control unit, and an air-fuel ratio control unit. A hydromechanical overspeed governor is incorporated in the fuel pump. The barometric flow control unit is designed to maintain selected speed for varying altitudes and forward speeds. Engine speed is manually selected with a rotary throttle control incorporated in the control unit. The air-fuel ratio control limits fuel flow to a maximum with relation to air mass flow over a critical engine range and prevents overfueling the combustion chamber during rapid acceleration and at high altitudes.

The engine-inlet installation and supporting framework were mounted on the suspended platforms of three thrust stands designed for supporting and measuring the thrust of an airplane. Thrust was measured with load cells mounted on the two larger stands normally used to support the two main gears of an airplane.

Description of Inlet

The inlet was designed as an axisymmetric external-internal compression type having a conical centerbody with an apex half-angle of $12\frac{1}{2}^{\circ}$. The design Mach number was 3.0; the design centerbody position, however, placed the conical shock wave slightly ahead of the leading edge at $M = 3$ to allow some tolerance for a centerbody positioning system to operate without allowing the conical shock to enter the inlet. The cowl lip was relatively sharp and had a ratio of lip radius to cowl-leading-edge radius of approximately 0.007. A drawing and ordinates of the internal arrangement of the inlet are presented in figure 2 and the internal area distribution is shown in figure 3. The ordinates for the internal contours are presented in table I.

TABLE I.- INTERNAL CONTOUR OF THE INLET

x		r_b		r_c	
in.	cm	in.	cm	in.	cm
0	0	0	0		
20.780	52.78	4.603	11.69	8.750	22.22
24.720	62.79	$12\frac{1}{2}^{\circ}$ cone		8.750	22.22
25.156	63.90			8.741	22.20
25.594	65.01			8.733	22.18
26.031	67.12			8.728	22.17
26.469	67.23			8.724	22.16
26.906	68.35			8.706	22.11
27.344	69.45			8.689	22.07
27.781	70.56			8.663	22.00
28.219	71.68			8.636	21.94
28.656	72.79			8.610	21.87
28.875	73.34	6.388	16.22		
29.094	73.89	6.436	16.35	8.566	21.76
29.313	74.45	6.479	16.46		
29.598	75.27	6.598	16.76	8.453	21.47
30.188	76.68	6.628	16.84		
30.406	77.23	6.663	16.92		
30.625	77.79	6.694	17.00		
31.000	78.74			8.325	21.15
31.063	78.89	6.738	17.11		
31.281	79.45	6.755	17.16		
31.500	80.00	6.764	17.18		
31.719	80.57	6.773	17.20		
31.938	81.13	6.781	17.22		
32.000	81.28			8.180	20.77
32.156	81.68	6.781	17.22		
32.375	82.23	6.764	17.18		
32.594	82.79	6.751	17.15		
32.813	83.35	6.720	17.07		
33.031	83.90	6.694	17.00		
33.250	84.46	6.650	16.89	8.009	20.34
34.000	86.36	Straight line		7.924	20.13
35.000	88.90			7.825	19.88
36.000	91.44			7.735	19.65
37.000	93.98			7.658	19.45
38.000	96.52			7.586	19.27
39.000	98.06			7.520	19.10
40.000	101.60			7.458	18.94
41.000	104.14			7.400	18.80
42.000	106.68			7.346	18.66
43.000	109.22			7.298	18.54
44.000	111.76			7.252	18.42
45.000	114.30			7.230	18.86
46.000	116.84			7.225	18.25
46.750	118.75			7.230	18.36
47.000	119.38			7.235	18.38
48.000	121.92			7.270	18.47
49.000	124.46			7.322	18.60
49.900	126.75	4.000	10.16		
50.000	129.00	Straight line		7.417	18.84
51.000	129.54			7.514	19.09
52.000	132.08			7.618	19.35
53.000	134.62			7.724	19.62
66.300	168.40			9.125	23.17
94.000	238.76	4.000	10.16	9.125	23.17

The engine was also operated with a cowl-lip modification which consisted of the addition of a rounded leading-edge fairing to the original sharp cowl lip. The rounded leading edge was essentially an NACA 1-40-200 nose inlet, defined in reference 3 with the internal contour as applied in reference 4. The ordinates for the rounded nose are presented in table II.

TABLE II.- CONTOUR OF ROUNDED LEADING EDGE

x		r_c		r_d	
in.	cm	in.	cm	in.	cm
17.780	45.16	10.06	25.55	10.06	25.55
18.280	46.48	9.32	23.77	10.67	28.10
18.780	47.70	9.09	23.09	10.90	28.69
19.280	48.67	8.93	22.68	11.05	28.07
19.780	50.24	8.83	22.43	11.15	28.32
20.280	51.86	8.76	22.25	11.21	28.47
20.780	52.78	8.75	22.22	11.25	28.67

The inlet was designed to be attached to the turbojet engine previously discussed to provide the required airflow under the static test conditions and had a cowl leading-edge diameter of 17.5 inches (44.45 cm). No attempt was made to simulate the external shapes of a nacelle, although the outside of the leading edge was smooth for a short distance back from the leading edge. The photograph of figure 1 shows the general external arrangement of the engine-inlet combination.

The mechanical design of the model provided for fore-and-aft translation of the centerbody from 2 inches (5.08 cm) aft ($\Delta x = -2$) to 14 inches (35.56 cm) forward ($\Delta x = 14$) of the design position. The airflow characteristics of the engine were such that sonic flow could be attained over a range of Δx from almost 4 inches (10.16 cm) to -2 inches (-5.08 cm).

Three auxiliary intake doors were located as shown in figure 2, section A-A. The doors were hinged at the downstream edge and opened outward, the operating mechanism being linked together to provide simultaneous operation of all three doors. The doors were used in order to provide a means of bypassing the inlet to supply more air rapidly to the engine should it become necessary to unchoke the inlet rapidly.

Instrumentation

Engine instrumentation.- Instrumentation used for operating and measuring the performance of the engine included a percentage speed indicator, jet pipe temperature indicator, thrust indicator, flowmeter, vibration level indicator, and ambient temperature and pressure indicators. A percentage speed indicator which consisted of a commercial digital frequency sensor actuated by an engine-driven tachometer generator was used to indicate engine rotational speed in increments of 0.1 percent. Chrome-alumel thermocouple sensors located in the jet pipe together with a galvanometer provided measurements of exhaust-gas temperatures. The thrust indicator consisted of two parallel-connected

1000-pound (4448 newtons) strain-gage load cells whose output was indicated on a single millivolt meter. A turbine flowmeter was used to measure fuel flow. The vibration level indicator consisted of velocity-type vibration pickups mounted on the engine in combination with a vibration analyzer. A self-balancing potentiometer connected to a thermocouple under the lip of the engine inlet was used to measure inlet air temperature. Ambient air pressures were obtained from local weather station measurements.

Inlet instrumentation.- Total-pressure distribution and recovery at the exit of the inlet were obtained by rotating the rake at the location shown in figure 2. Static orifices were located on the rake, on the centerbody rotating with the rake, and on the outer duct wall, all in the plane of the total-pressure rakes. Rotation of the rake covered 240° at approximately 6° to 8° per second. Although data were recorded continuously as the rake rotated, the data were analyzed for discrete rake positions located 45° apart. Since the spacing of the total-pressure tubes was such that a numerical average of the pressures was equivalent to area weighting of the pressures, the total-pressure recovery was computed as the average of the readings of all tubes at each rake position. To reduce the effects of lag in the pressure readings, data were included with the rake traveling in both directions. Static orifices were located along the top center line of the outer duct and centerbody surface in the region of the throat (fig. 2). These orifices were connected to a manometer board and were used to observe the existence and region of supersonic flow in the duct. No data from these orifices are presented. The four orifices at station 33.0 were used to determine the engine speed required to choke the inlet and the corresponding total-pressure ratio at each centerbody position at which choking at the inlet throat could be achieved.

Noise instrumentation.- The microphones used for the external noise measurements were commercially available condenser microphones with a 5/8-inch-diameter (1.59 cm) diaphragm used with parallel impingement, and the output signals were recorded on a multichannel direct-recording tape recorder. The overall response of the system from 20 cps to 10 000 cps, considered adequate to record the blade-passage frequency, was flat within ±2 dB. The measurements were taken on both a 25-foot- (7.62 m) and a 70-foot- (21.34 m) radius circle as shown in the planview of figure 4 and were made in accordance with the recommendations of reference 5. Only the data from the 25-foot- (7.62 m) distance measurements are included since they are representative and have a higher signal-to-noise ratio. The internal measurements were taken with two sintered bronze microphones which were flush-mounted inside the wall of the inlet at the axial stations shown in figure 2. The microphone at station 25.00 was ahead of the shock region, and the microphone at station 45.00 was behind the shock region. For purpose of analysis, the tape recordings were played back into a graphic level recorder, a one-third-octave band wave analyzer, and a narrow-band wave analyzer.

Test Procedures

The tests were made for a range of engine rotational speeds from idle to 100-percent rated speed. Engine speed for each run was held nearly constant for from 1 to 2 minutes during which time performance, pressure, and sound measurements were made. Tests were made with inlet centerbody positions varying from 2 inches (5.08 cm) behind to 14 inches (35.56 cm) ahead of the Mach 3 design position. In order to obtain a reference, tests were also made with the inlet doors open. Density of the fuel (grade JP-4) was measured prior to each series of runs.

DISCUSSION OF RESULTS

Engine Performance

Values of exhaust gas temperature, thrust, fuel flow, and specific fuel consumption for various rotational speeds are given in figures 5 to 12. Performance values with inlet doors open are given in figures 5 to 8. All values given in the engine performance figures are for the sharp-leading-edge inlet and have been corrected to standard temperature and pressure. The results shown for the various centerbody positions indicate that with inlet doors open, engine performance was unaffected by centerbody position. Test results not shown indicated no engine performance variation with door opening for positions from half open to the full open position. Figures 5 to 8 show good correlation of measured values with engine speed and faired lines through the measured values are used as references for subsequent figures with the inlet doors closed.

Exhaust gas temperature.- Exhaust gas temperature (T_e) variations with engine rotational speed for various centerbody positions with the inlet doors closed are shown in figure 9. Shaded symbols are used to indicate tests with the inlet choked. For each centerbody position at which choking occurred, $\Delta x = -2, -1, 0, 1,$ and 2, an abrupt and rapid increase in exhaust gas temperature is shown for increases in engine speed above the lowest speed at which the inlet choked. The temperatures reached the maximum allowable value and further speed increases over the normal operational range could not be made. For the smallest throat area configuration, $\Delta x = -2$, with the inlet choked a temperature rise of about 250° C occurred for an engine speed increase from 70 percent to 80 percent compared with a normal temperature increase of about 50° C for this speed change with the inlet doors open. The engine rotational speed at which the inlet first choked and the maximum speed at which the highest allowable temperature was reached were progressively higher for centerbody positions which corresponded to larger inlet areas.

In addition to the abrupt temperature rise which accompanied choking, figure 9 shows that some increase in exhaust gas temperature for the closed-door configuration occurred throughout the engine speed range. The largest increases for the nonchoked closed-door configuration, 75° C and 50° C, occurred for the centerbody in the two most forward positions, Δx = 10 in. (25.4 cm) and 14 in. (35.56 cm).

Thrust.- The variation of engine thrust with rotational speed for different centerbody locations is shown in figure 10. Although some losses are evident for all tests with the inlet choked, the losses became much larger for each centerbody location as engine speed was increased above the value at which the inlet first choked for that particular centerbody location. Thrust losses as great as 20 percent of the inlet-doors-open value are indicated for operation with the inlet choked. Thrust was rapidly restored to the unchoked level when the inlet doors were opened.

Substantial thrust losses are also indicated for tests at high engine speeds with unchoked closed-door inlet configurations. Thrust losses as high as 15 percent of the open-door value occurred for the two maximum area configurations, Δx = 10 in. (25.4 cm) and 14 in. (35.56 cm). These losses are associated with total-pressure ratio and are discussed under inlet performance.

Fuel flow and specific fuel consumption.- The variation of fuel flow and specific fuel consumption with engine speed are shown in figures 11 and 12, respectively. A greater fuel flow with the inlet doors closed than with the doors open is shown in figure 11. The greatest increase occurred for the choked inlet with the centerbody in the rearward positions (Δx = -2, -1, and 0) corresponding to the three smallest throat areas. Variations for other centerbody locations were comparatively small. The greatest increase, about 13 percent, in fuel consumption is shown for the choked inlet with the smallest throat area, Δx = -2.

Specific fuel consumption was greater for the doors closed than for the doors open over most of the engine speed range (fig. 12). Increases are greatest for rearward centerbody locations with small throat areas for which there was both a loss in thrust and an increase in fuel consumption. An increase of up to 44 percent over the specific fuel consumption with the doors open is shown for the choked smallest throat area configuration. Increases are also shown for the unchoked closed-door configuration.

Engine vibration.- Instrumentation for detecting and analyzing engine vibrations indicated no measurable increase in engine vibration level for operation with the inlet choked.

Inlet Performance

Effect of engine speed on inlet total-pressure ratio.- Figure 13(a) shows that with the auxiliary doors open, the averaged inlet total-pressure ratio $\frac{\overline{p_t}}{p_a}$ varied from about 0.99 at low engine speeds to about 0.97 at the maximum engine speed attained, with little effect of centerbody position. In figure 13(b), with the auxiliary doors closed, choking could be attained only for a range of centerbody positions tested from $\Delta x = -2$ to $\Delta x = 2$. The total-pressure ratios at which choking first occurred are indicated by the dashed line. With the inlet unchoked, and at a constant engine speed, the total-pressure ratio increased with forward movement of the centerbody up to about $\Delta x = 4$; however, at more forward centerbody positions, the total-pressure losses increased because of higher velocities and subsequent losses at the sharp leading edge. The flagged symbols for the data at $\Delta x = 0$ and $\Delta x = -2$ indicate runs for which the auxiliary doors were sealed to prevent leakage. The leakage that existed with the doors unsealed tended to increase the mass flow into the inlet and was similar in effect to moving the centerbody a small amount to cause a small increase in the throat area.

The total-pressure ratio at which $M = 1$ first occurs at the inlet minimum was found to be essentially constant at a value of approximately 0.93 for the range of centerbody positions at which $M = 1$ could be attained ($\Delta x = 4$). Further increases in engine speed above that required to choke the inlet cannot result in greater losses in total pressure upstream of the inlet minimum because the velocity cannot be further increased. The increased airflow which is required by the engine can only be attained by an increase of the total-pressure losses downstream of the minimum. Therefore, the normal shock moves downstream in the expanding duct to where the local supersonic Mach number is that which provides the required shock losses. Operation in the region of high normal-shock losses can be avoided, however, by proper positioning of the centerbody, although keeping a region of supersonic flow at the inlet minimum would require the total-pressure ratio to be below 0.93. Thus, the total-pressure ratio corresponding to $M = 1$ is the primary measure of inlet performance since it represents the maximum total-pressure ratio at which the inlet can be operated with supersonic flow at the inlet throat.

Effect of engine speed and centerbody position on flow distribution.- Total-pressure distributions at the rake station for several centerbody positions are presented in figures 14 and 15. Figure 14 shows the effect of engine speed on the total-pressure distribution for the centerbody position $\Delta x = 0$, with the auxiliary doors closed. Generally, the circumferential variation was small; however, the radial variation was as much as ±3 percent of the average total-pressure ratio except for a value of $\frac{N}{N_{std}\sqrt{\theta}} = 0.83$ where the data indicate flow separation near the outer surface of the duct. Figures 15(a) and 15(b) show the effect of engine speed on the total-pressure distribution for the centerbody

positions of $\Delta x = -2$ and $\Delta x = 4$ with the auxiliary doors open and closed. At $\Delta x = -2$ the radial total-pressure distribution was flatter, as shown in figure 15(a). At this centerbody position, the velocity at the inlet leading edge was less than that for $\Delta x = 0$ (see fig. 14) and the adverse effects on the radial distribution have been reduced. At $\Delta x = 4$ (fig. 15(b)) the inlet could not be choked and the result was increased circumferential flow distortion. With the auxiliary doors open (figs. 15(a) and 15(b)), both radial and circumferential distortion were present and showed no effect of centerbody position.

Effect of leading-edge shape on inlet total-pressure ratio and flow distribution.- The total-pressure data presented in figure 16 show that the addition of the rounded leading edge increased the total-pressure ratio as much as 0.04 at $\Delta x = 0$. Although the data at $\Delta x = 2$ show a much smaller difference in total-pressure ratio, the sharp-leading-edge data are for the auxiliary doors unsealed. An estimate of the decrease in total-pressure ratio from the $\Delta x = 0$ and $\Delta x = -2$ data of figure 13 indicates that the sharp lip losses at $\Delta x = 2$ would be of the same magnitude as that for $\Delta x = 0$. At $\Delta x = 14$, although only one data point was taken, the total-pressure ratio was very high compared with the sharp-lip data at the same centerbody position. The large difference in total-pressure ratio between the sharp and rounded leading edges at $\Delta x = 14$ verifies that the low total-pressure ratio of the sharp-leading-edge configuration with the centerbody in the extreme forward position was due to large separation losses at the leading edge. The total-pressure distributions presented in figure 17 for $\Delta x = 0$ and 2 show very little radial or circumferential distortion compared with the sharp-leading-edge data of figures 14 and 15. This result indicates that the low velocities near the outer wall with the sharp leading edge can be attributed to the adverse effects of the sharp leading edge.

Effects of auxiliary doors on inlet total-pressure ratio and flow distribution.- Operation of the inlet choked resulted in a loss of available thrust and the centerbody translation was relatively slow; therefore, rapid-opening auxiliary doors were tested as a means to provide rapid increase in thrust. Of concern in such a system would be the effect on flow distribution at the compressor should one or more of the auxiliary doors fail to open and cause asymmetrical entry of the auxiliary airflow. Presented in figures 18 and 19 are the results of tests made with one door open and two doors open. The total-pressure-ratio data (fig. 18) are shown compared with the all-doors-closed and all-doors-open data from figure 13. Opening one door unchoked the inlet and reduced the total-pressure losses and allowed a maximum engine speed to be attained equal to that with all three doors open, although the total-pressure ratio was less than that for all three doors open. Opening the second door resulted in total-pressure-ratio values about midway between those for one door open and all three doors open. The total-pressure distributions presented in figure 19 show that with one door open, at both maximum and moderate (about 86 percent) engine speeds, the total-pressure distributions were rather flat in the radial

direction, whereas the circumferential distributions were flat with the exception of the data at 180° and 225° at maximum engine speed and indicated a higher total-pressure ratio. It should be noted that the open door extended from 85° to 145° of the duct circumference. With two doors open, the circumferential total-pressure variations were more gradual at moderate engine speeds, although the variation of total-pressure ratio was about the same as with one door open. At the maximum engine speed, the circumferential variation of total pressure was less with two doors open as compared with that for one door open.

Acoustic Performance

The results obtained on the effects of inlet flow choking on the noise emitted from the inlet by the compressor are presented in figures 20 to 26 for selected operating conditions. Comparisons are made of the radiated noise for choked and unchoked conditions. Data are presented for constant speed and different centerbody positions, and for different speeds and a constant centerbody position. Acoustic data are presented in the form of overall sound-pressure-level radiation patterns, fundamental-frequency radiation patterns, and one-third-octave band frequency analyses.

Far-field overall sound-pressure-level radiation patterns.- Acoustic radiation patterns of the overall sound-pressure level measured at a 25-foot radius are presented in figures 20 and 21 for two different engine speeds. Figure 20 presents the data taken at 84.7-percent speed with the sharp inlet configuration and a centerbody position of $\Delta x = 0$ for choked flow operating conditions, compared with a centerbody position of $\Delta x = 14$ for unchoked flow conditions. The overall noise level with the inlet choked is 2 to 5 dB less than with the inlet unchoked in the quadrant forward of the engine, the greatest reduction occurring near the 30° azimuth and the least reduction occurring at the 90° azimuth. These noise reductions as a result of inlet choking were accompanied by approximately a 2.8-percent thrust loss (shown as approximately 25 lb in fig. 10).

Figure 21 presents similar data for a constant centerbody position of $\Delta x = -2$. For this comparison it was necessary to make use of data for engine speeds of 67.4 percent (unchoked) and 71.2 percent (choked). The data again show that the choked condition produces lower overall noise levels than the unchoked condition even though the speed and thrust level are higher. It should be noted that the speed for the unchoked case is about 5 percent less than that for the choked case. This result means that the flow velocities in the restricted portion of the inlet are relatively high even though choking has not occurred. The results suggest that some noise reduction might be obtained just because of the existence of such high velocity flows; however, the present tests were not definitive enough to evaluate such an effect.

Far-field one-third-octave band spectrum analyses.- Figure 22 illustrates one-third-octave band spectral analyses of measurements taken at the 30° azimuth on the 25-foot radius at the same operating conditions as for figure 20. Sound-pressure levels for choked and unchoked conditions are plotted against frequency. The noise spectrum for the unchoked condition shown in figure 22 exhibits peaks in the frequency range above 5000 cps. These peaks are associated with discrete tones at the blade-passage frequencies and higher harmonics. It may be noted that the peaks associated with these discrete tones are not evident for the choked condition. The broad-band noise levels below about 5000 cps are seen to be about the same for both the choked and unchoked conditions. Similar results are obtained in figure 23 for the choked and unchoked conditions at the lower engine speeds shown in figure 21 (constant centerbody positions).

Far-field fundamental-blade-passage-frequency radiation patterns.- To examine further the effects of choking described in figures 22 and 23, the data of figures 20 and 21 were analyzed at the fundamental-blade-passage frequency by means of a 50-cps bandwidth filter. The results are shown in figures 24 and 25. In figure 24 it can be seen that noise level reductions were obtained at all azimuth angles in the front quadrant. Reductions of the order of 20 dB were obtained for azimuth angles from 0° to about 45°. Smaller reductions occurred at the larger azimuth angles. Very similar results are shown in figure 25 for lower speed conditions and for a constant centerbody location.

Effects of inlet lip fairing for a choked and unchoked condition at nearly equal thrust.- Studies similar to those described in figures 20 to 25 were performed during operation of the engine with the faired inlet lip shown in figure 2. The data were analyzed to compare choked and unchoked inlet flow conditions with the engine at nearly equal thrust (1.5-percent thrust difference). The engine speeds were slightly higher and the centerbody positions were different than the operating conditions of figure 20. The results which are summarized by the one-third-octave band spectrum analyses of figure 26 show that although the absolute sound-pressure-level values were different, the general trends of the data were the same as described in figures 20 to 25 – choking the inlet flow reduced the noise emitted from the front of the inlet, particularly the discrete tones associated with the fundamental blade-passage frequency.

The main difference noticed was that the peak associated with the fundamental blade-passage frequency was not as pronounced as with the sharp inlet; this difference suggests that this peak is partially caused by the compressor blades passing through the turbulent flow generated by the sharp inlet.

One-third-octave spectrum analyses inside the inlet.- A sample of the measurements taken inside the inlet with the flush-mounted sintered-bronze microphones is shown in figure 27. The data shown are for the same engine and inlet conditions as for figure 21. The results obtained for the microphone mounted forward of the shock region are shown

in the top half of the figure; those for the aft microphone location are shown in the lower half. These spectra contain broad-band and discrete frequency components as do those of figures 22 and 23. The forward microphone trace for the unchoked condition shows some relatively strong peaks associated with the blade-passage frequencies. As would be expected, the presence of the shock wave downstream of the microphone during choked flow operation essentially eliminates these high-frequency peaks. Choking has very little effect on the noise downstream of the shock wave as is shown by the data from the aft microphone.

OPERATIONAL CONSIDERATIONS

The results indicate that operation of the test engine at different rotational speeds with a choked inlet would require matching inlet throat area with engine speed. The need arises from the previously indicated variation of minimum choking speed with inlet area and the restriction of operations in the choked condition with a given inlet area to a narrow range of operational speeds. It has been shown that the usable range of engine speeds for the choked inlet with a given inlet area was between the lowest speed at which the inlet would choke and the maximum speed for which losses become unacceptable or temperatures were excessive.

Operations with the inlet choked during a landing approach would require some provision for quickly unchoking the inlet in case of an aborted landing or emergency. With the inlet in a choked condition, a rapid engine acceleration to the maximum engine rotational speed to obtain the high thrust values required would produce an unacceptable exhaust gas temperature rise. Rapidly unchoking the inlet had no apparent adverse effect on the test engine.

CONCLUDING REMARKS

An investigation has been conducted to determine the effects of inlet choking on inlet-engine performance and radiated inlet noise of a turbojet engine. Engine and inlet performance and noise measurements were made during tests with a small (1700-pound thrust) turbojet engine equipped with a supersonic inlet with throat area variable by means of a translating centerbody.

No increase in vibration of the test engine with the inlet choked was observed and no erratic engine behavior was noted when the inlet was rapidly unchoked.

For each centerbody location, some engine performance losses were incurred at the lowest speed at which the inlet choked and these losses increased rapidly as engine speed was increased above the choking speed for each centerbody location. Increases in exhaust

gas temperature to the maximum allowable value prevented increases in speed over the normal operational range.

For the range of centerbody positions at which the inlet could be choked, choking occurred at a value of total-pressure ratio of approximately 0.93.

For the range of centerbody positions tested, the maximum total-pressure ratio was found to occur at a centerbody position which placed the inlet minimum downstream from the inlet leading edge, although the resulting throat area was less than that for a more forward centerbody position.

Total-pressure loss and low velocities near the outer duct wall were found to result from the sharp leading edge with the centerbody located near the design position. As the centerbody was moved forward so that the inlet minimum was located near the leading edge, the losses became increasingly large.

With the centerbody at the design position, opening one or two auxiliary doors increased the total pressure and allowed maximum engine speed to be attained although operation with one door open resulted in increased circumferential flow distortion.

Noise measurements indicated that choking the inlet flow was beneficial in reducing the noise levels forward of the engine. Noise reductions of 2 to 5 dB were observed in the overall noise levels and 2 to 20 dB were observed in the noise levels of the fundamental-blade-passage frequencies, the smaller reductions occurring from the 45° to the 90° azimuth and the larger reductions occurring from the 0° to about the 45° azimuth.

Langley Research Center,
National Aeronautics and Space Administration,
Langley Station, Hampton, Va., December 14, 1966,
126-16-03-01-23.

REFERENCES

1. Sobel, J. A., III; and Welliver, A. D.: Sonic Block Silencing for Axial and Screw-Type Compressors. Noise Control Shock Vib., vol. 7, no. 5, Sept.-Oct. 1961, pp. 9-11.

2. Carmichael, R. F.: Analyses of Dynamic Measurements Obtained During the J79-13 Engine Installation Test for the NB-66D Laminar Flow Control Aircraft. Rept. NOR-62-163, Norair Div., Northrop Corp., July 1962.

3. Baals, Donald D.; Smith, Norman F.; and Wright, John B.: The Development and Application of the High-Critical-Speed Nose Inlets. NACA Rep. 920, 1948. (Supersedes NACA ACR L5F30a.)

4. Bryan, Carroll R.; and Fleming, Frank F.: Some Internal-Flow Characteristics of Several Axisymmetrical NACA 1-Series Nose Air Inlets at Zero Flight Speed. NACA RM L54E19a, 1954.

5. Anon.: Measurements of Aircraft Exterior Noise in the Field. ARP 796, Soc. Automotive Engrs., Inc., c.1965.

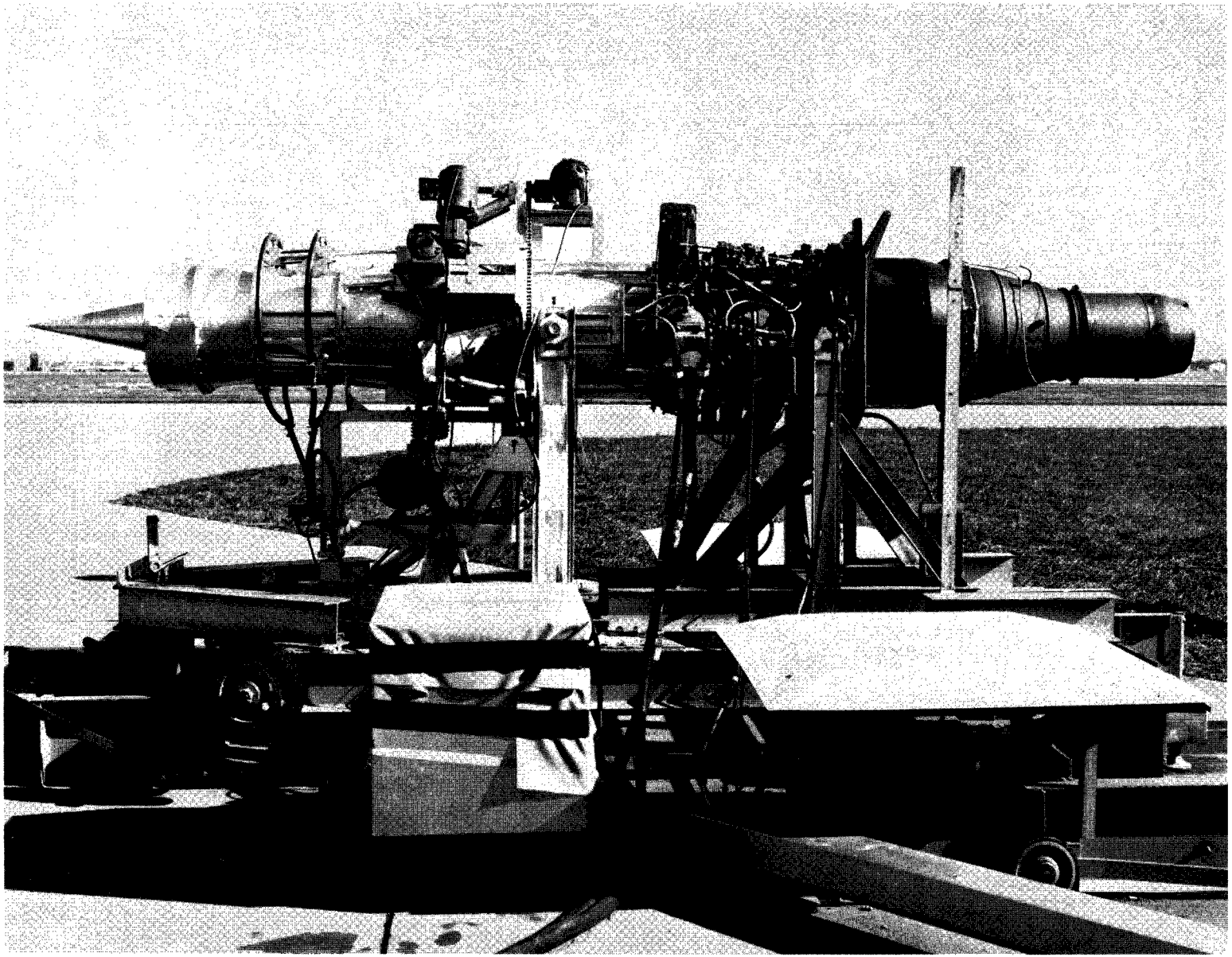

Figure 1.- Viper 8 jet turbine engine with three-dimensional supersonic inlet mounted on thrust stand. L-63-9553

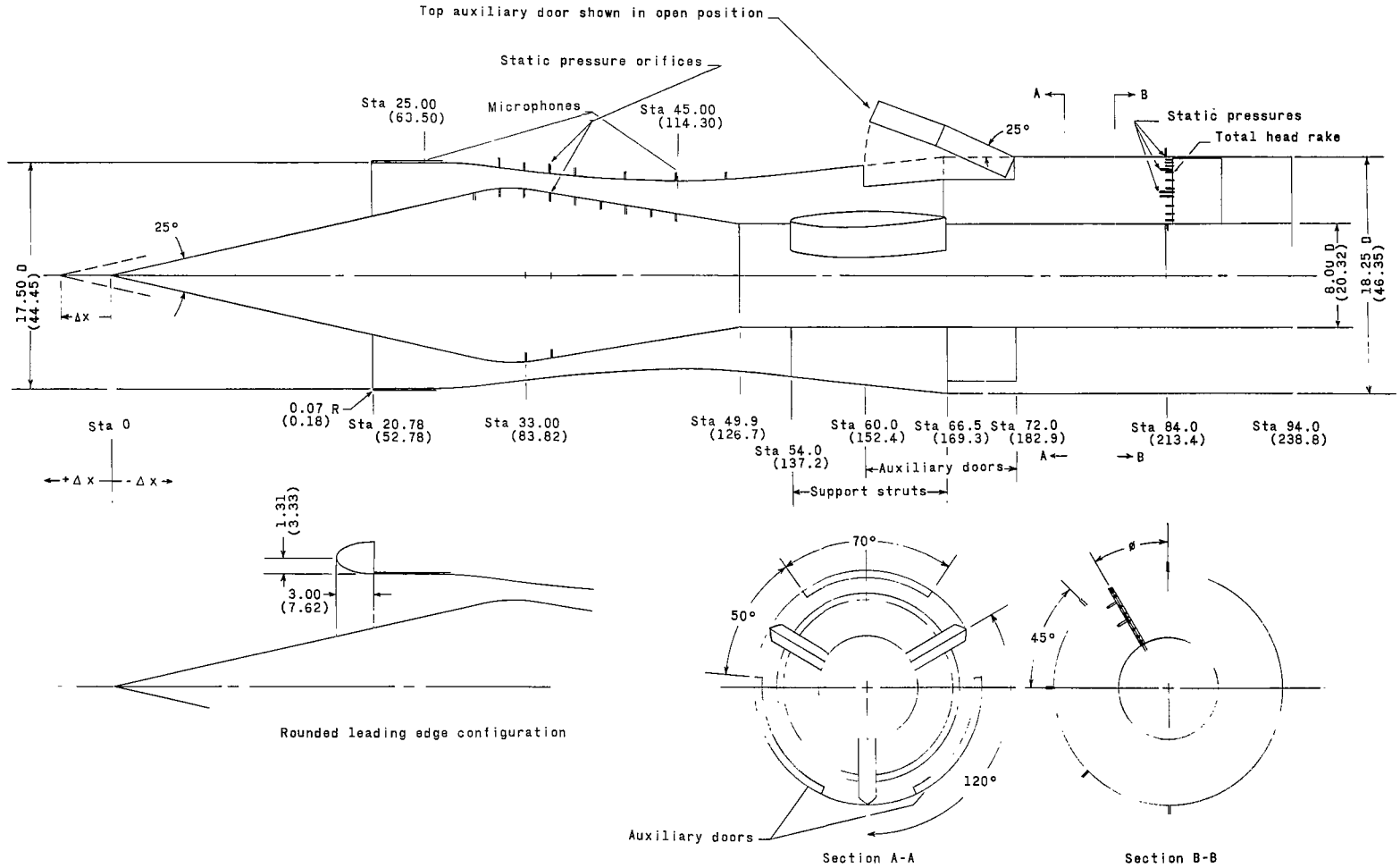

Figure 2.- Internal arrangement of inlet model. All dimensions are in inches unless otherwise noted. (Values within parentheses are in centimeters.)

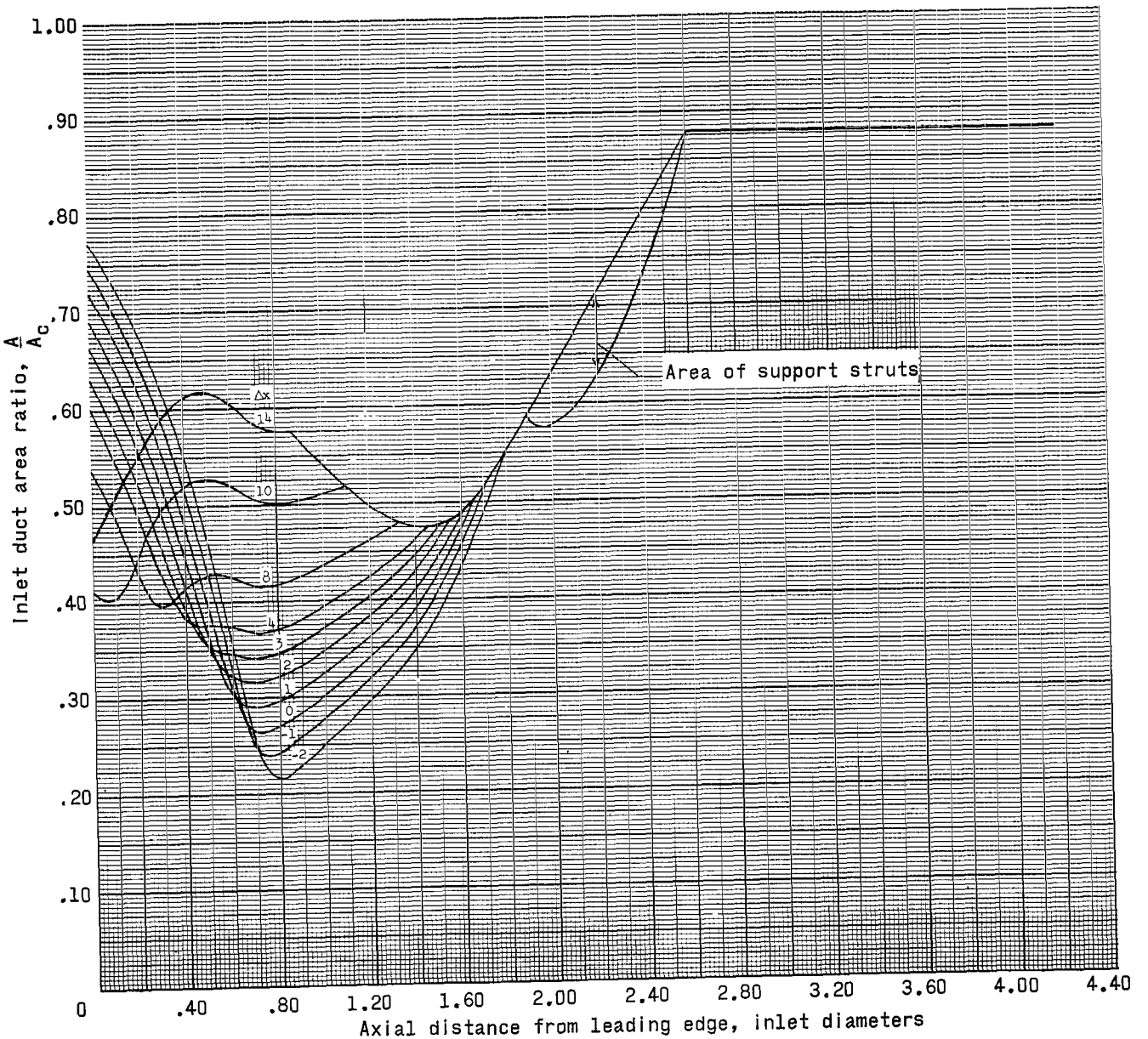

Figure 3.- Variation of inlet duct area.

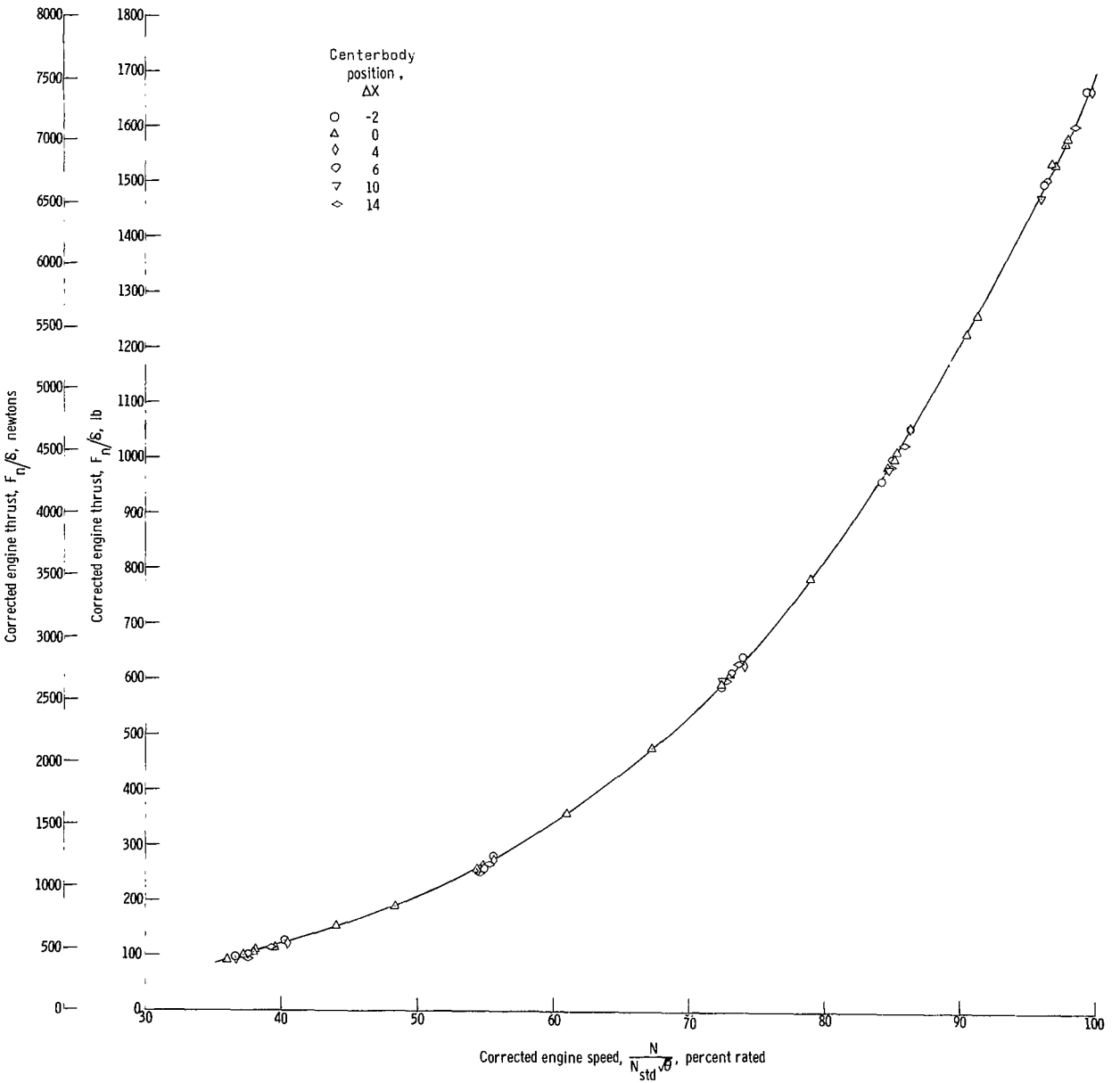

Figure 6.- Variation of thrust with engine speed for test engine with inlet doors open.

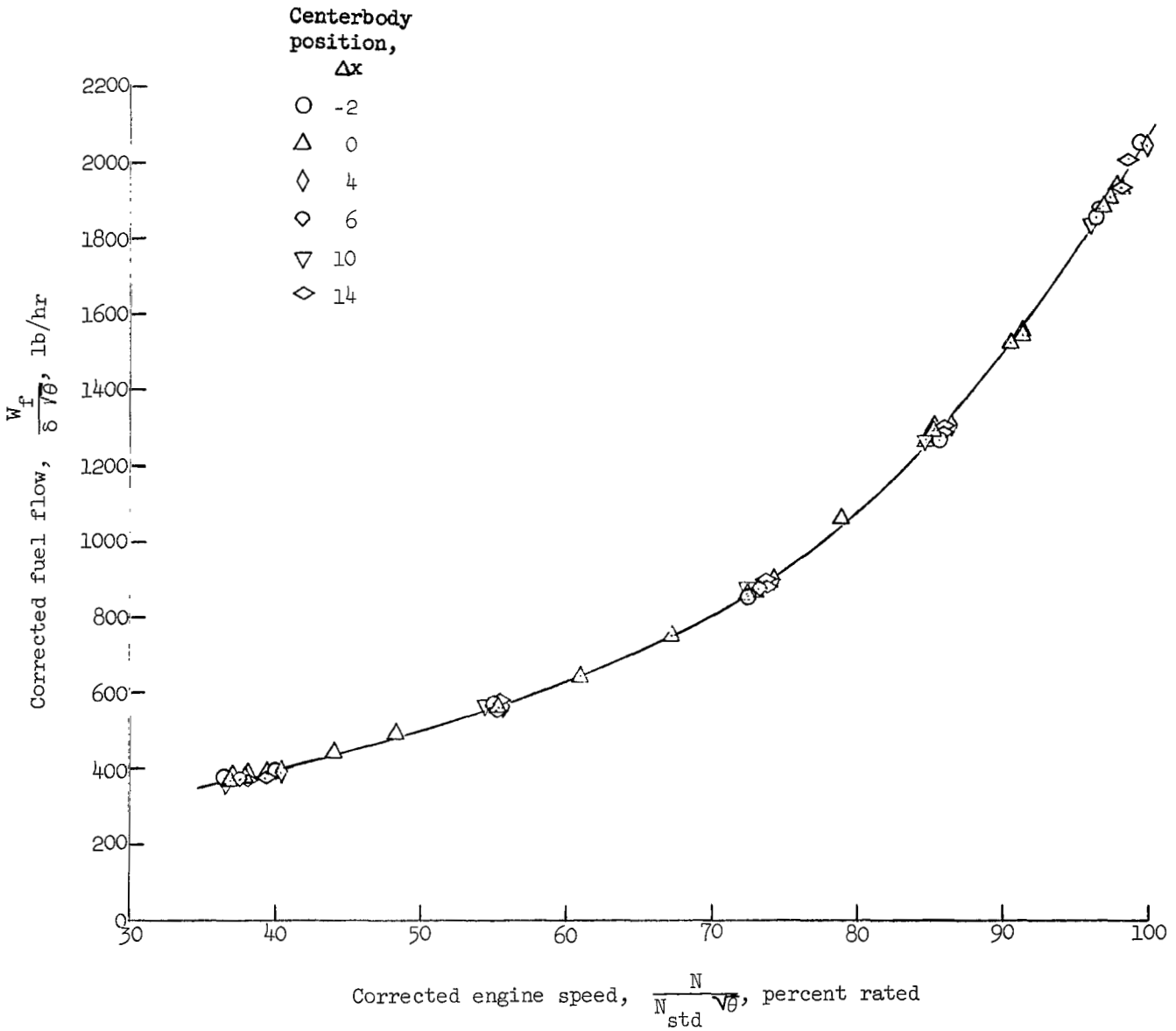

Figure 7.- Variation of fuel flow with engine speed for test engine with inlet doors open.

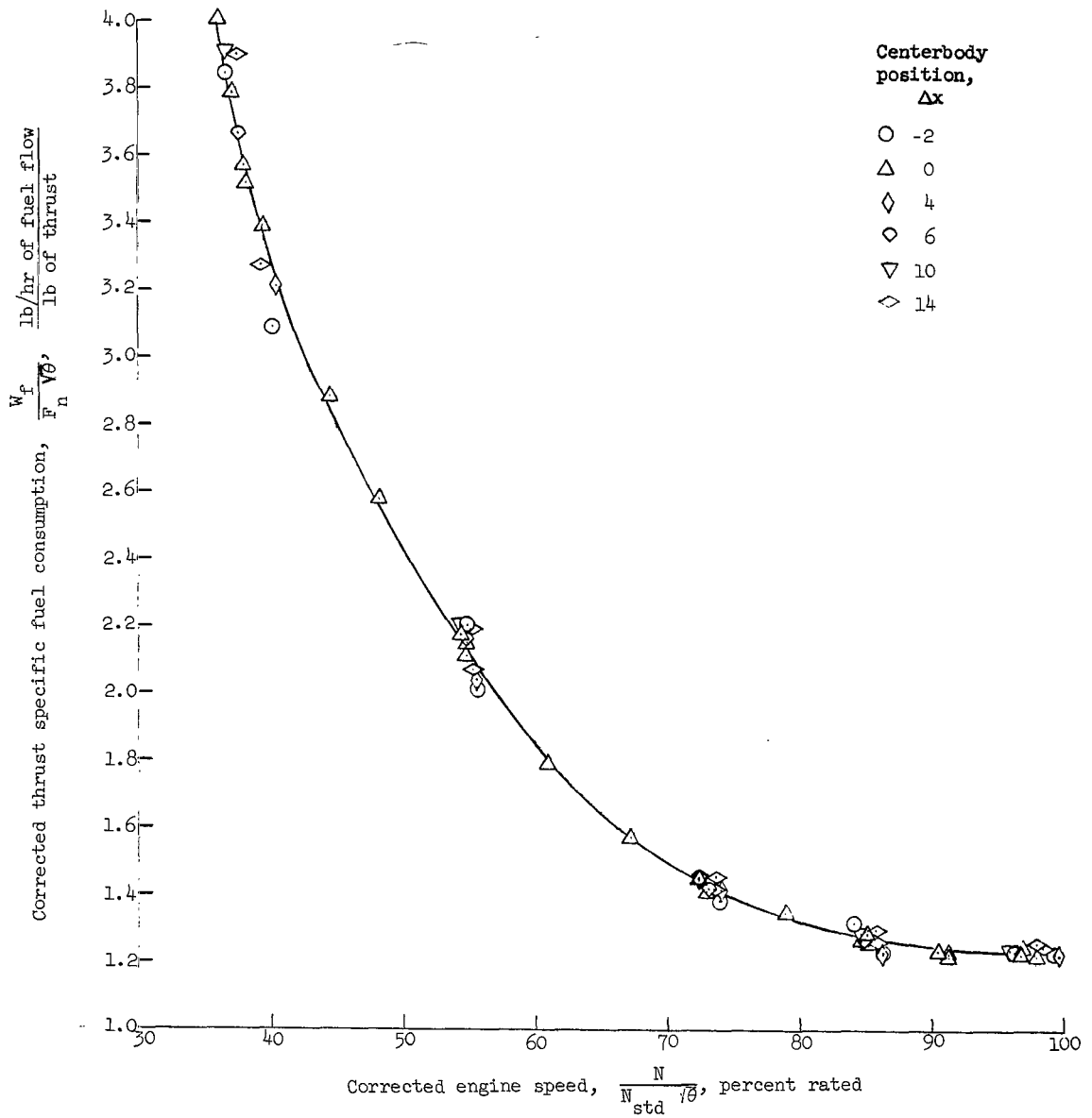

Figure 8.- Variation of specific fuel consumption with engine speed for test engine with inlet doors open.

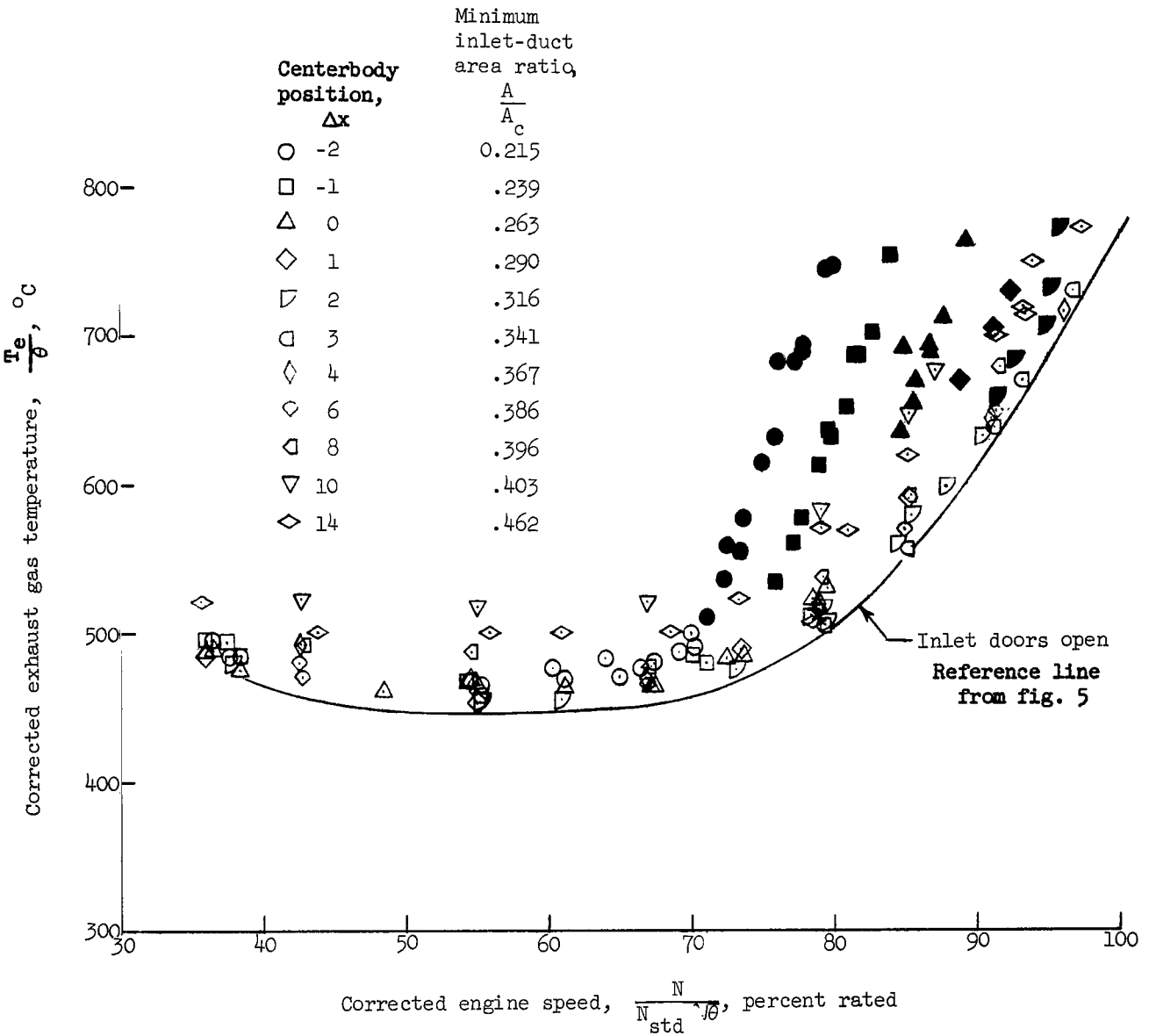

Figure 9.- Variation of exhaust gas temperature with engine speed for test engine with inlet doors closed. Solid symbols indicate choked inlet.

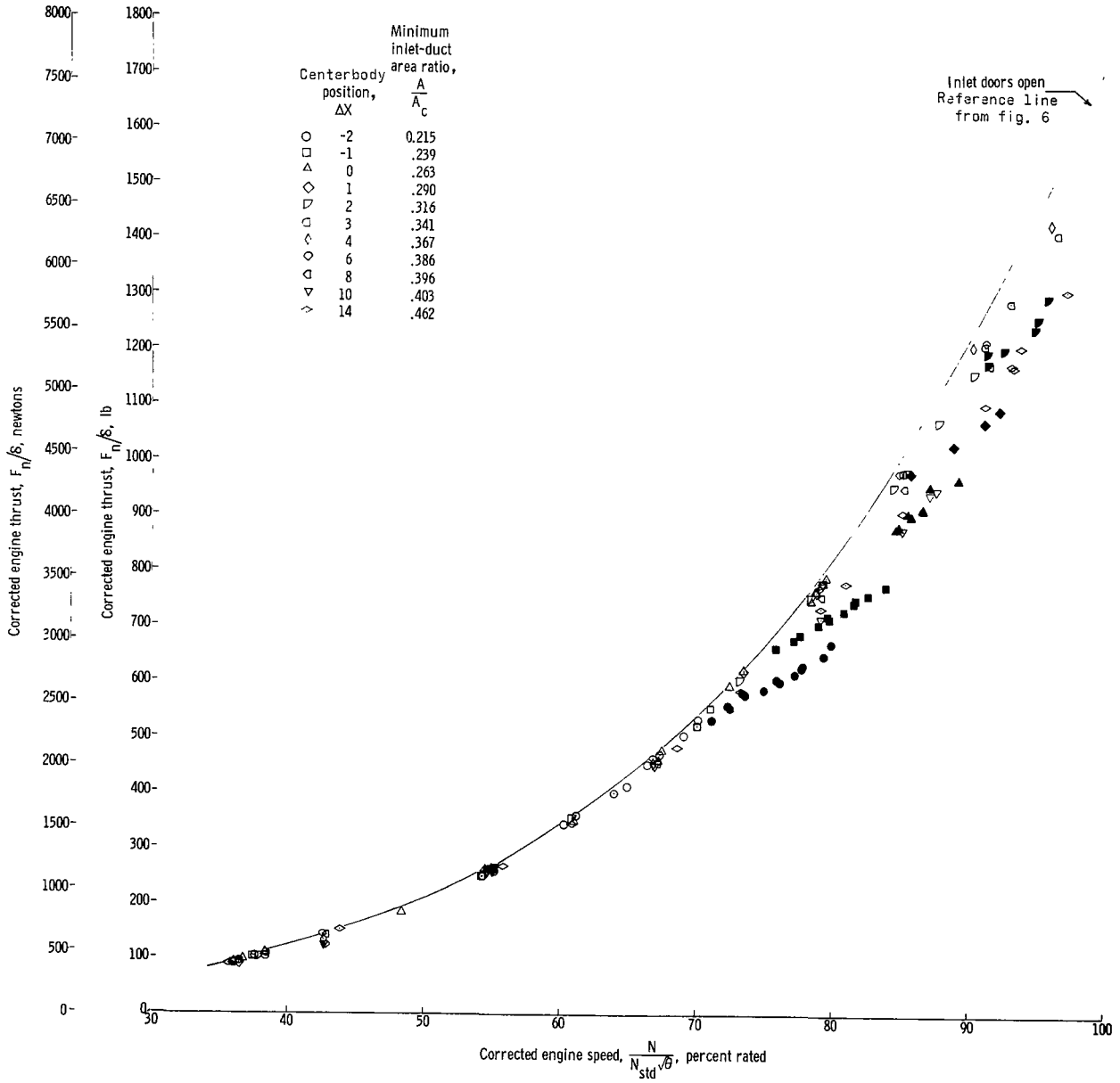

Figure 10.- Variation of thrust with engine speed for test engine with inlet doors closed. Solid symbols indicate choked inlet.

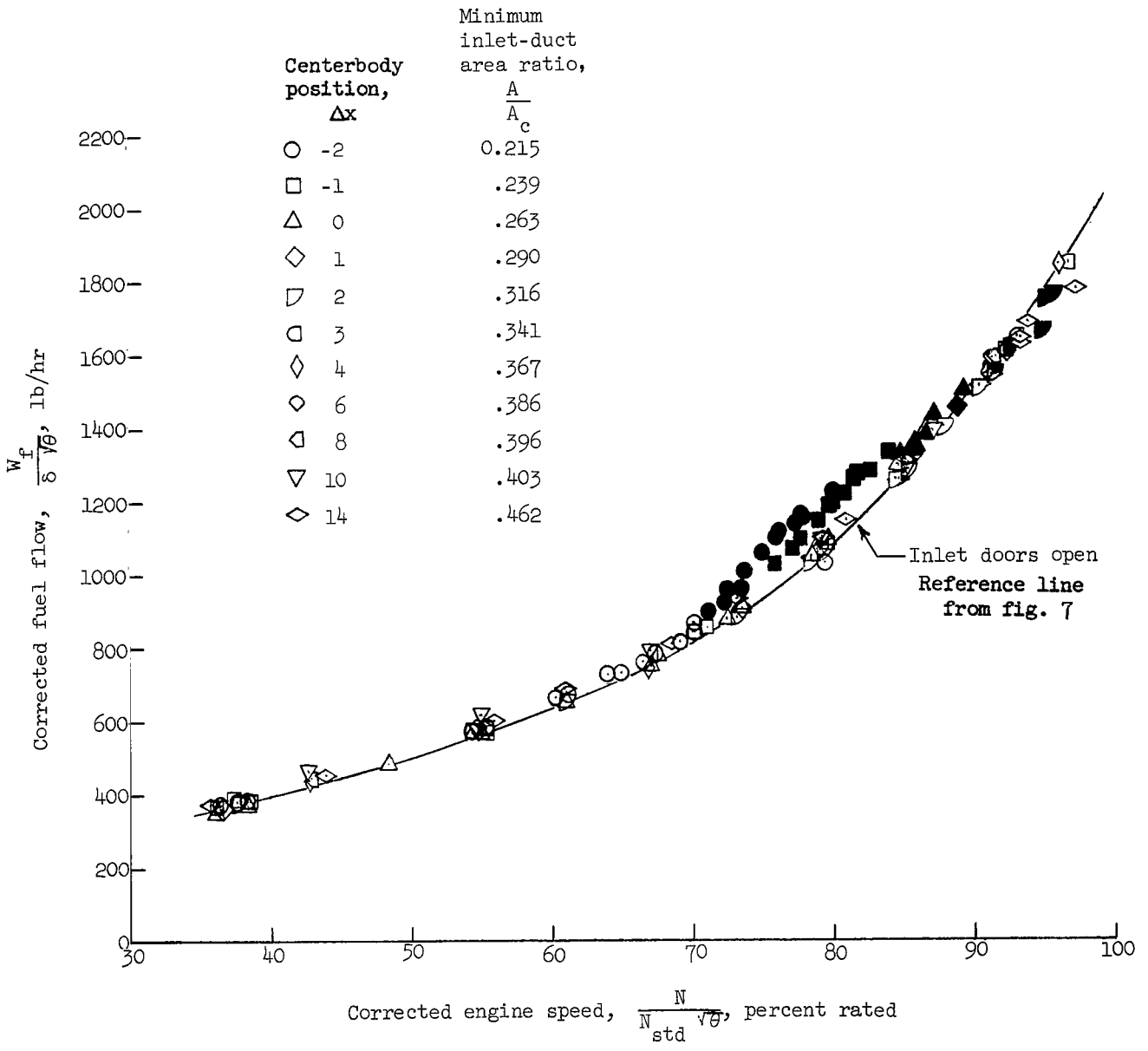

Figure 11.- Variation of fuel flow with engine speed for test engine with inlet doors closed. Solid symbols indicate choked inlet.

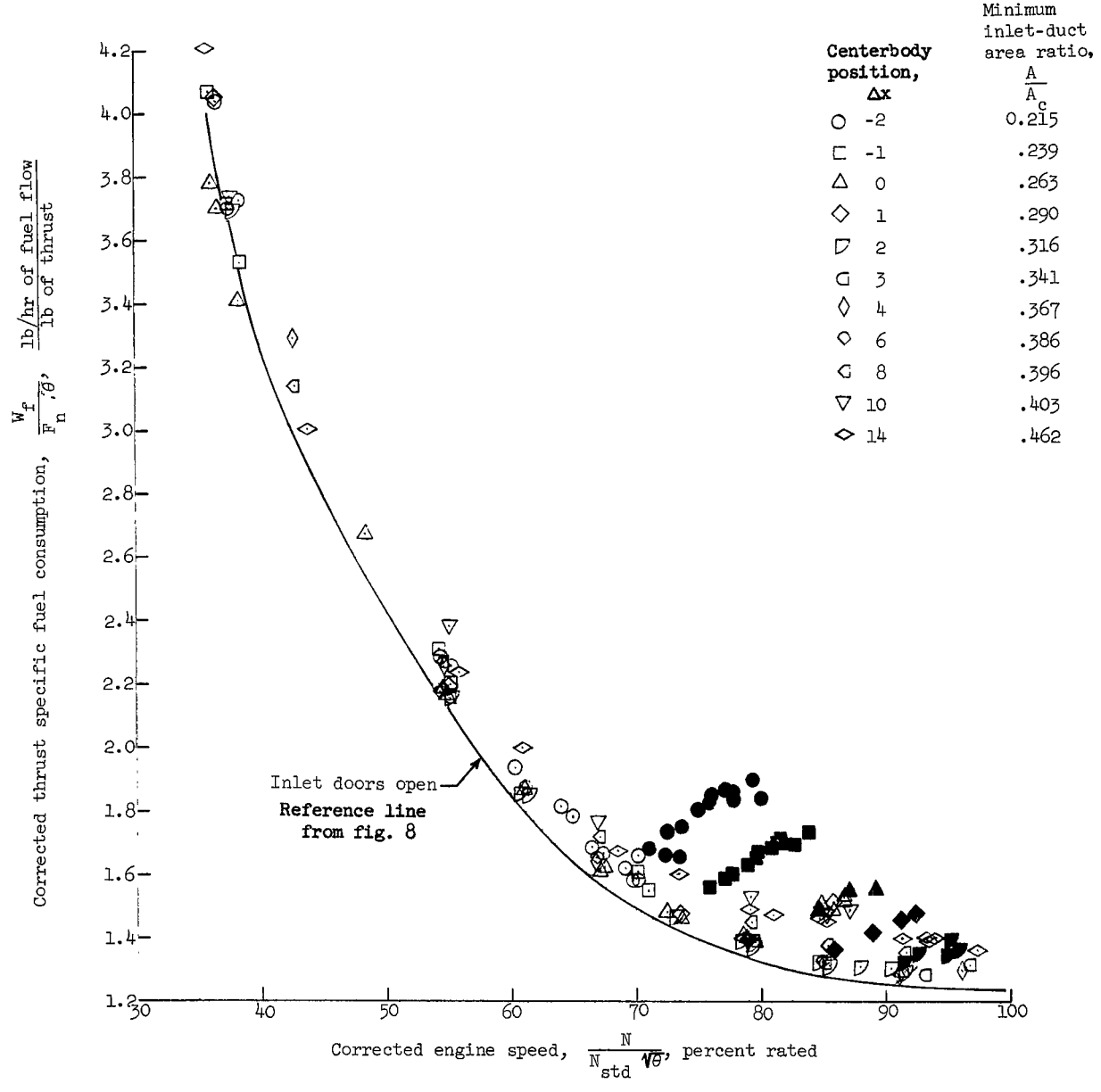

Figure 12.- Variation of specific fuel consumption with engine speed for test engine with inlet doors closed. Solid symbols indicate choked inlet.

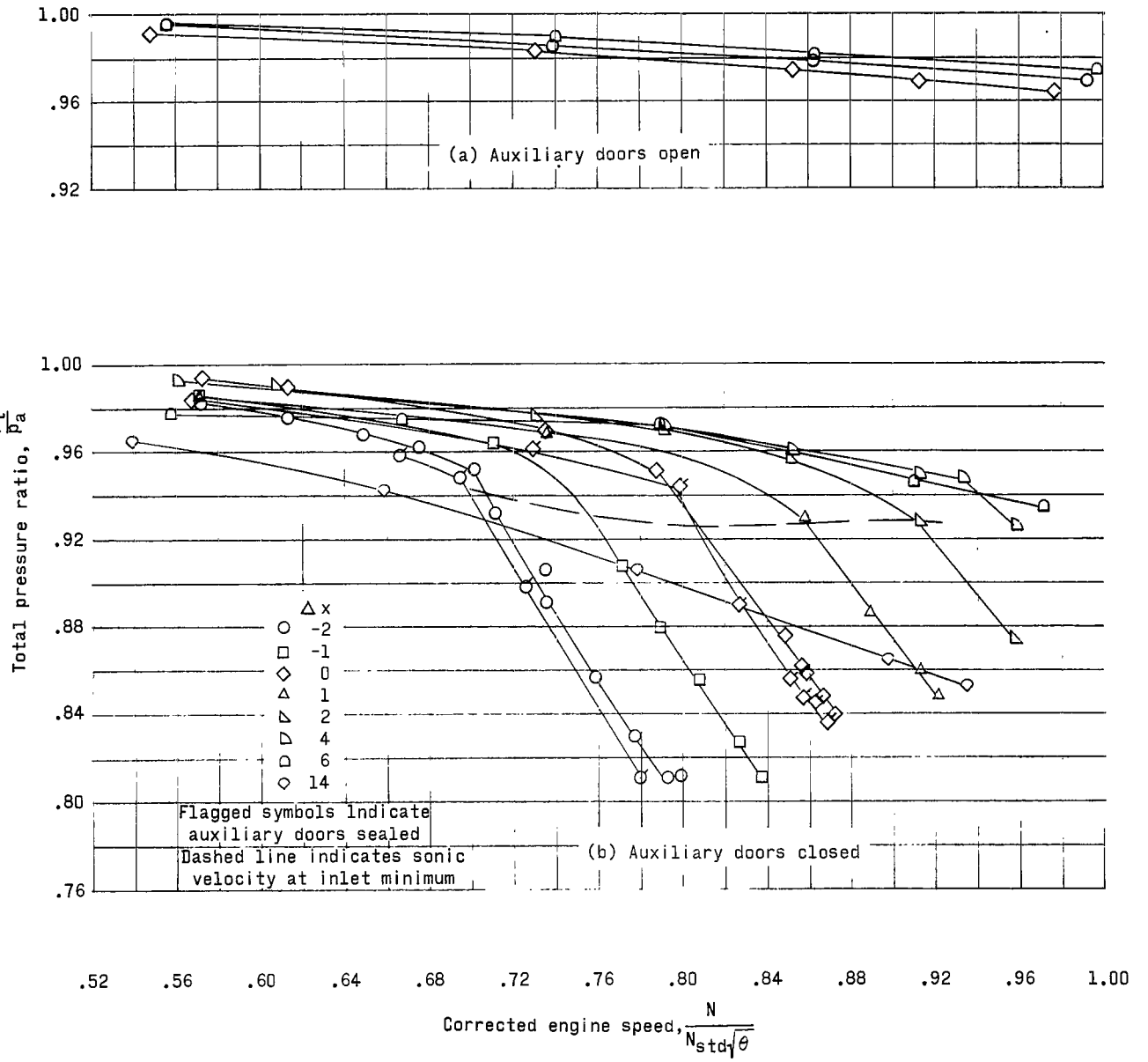

Figure 13.- Variation of inlet total-pressure ratio with corrected engine speed.

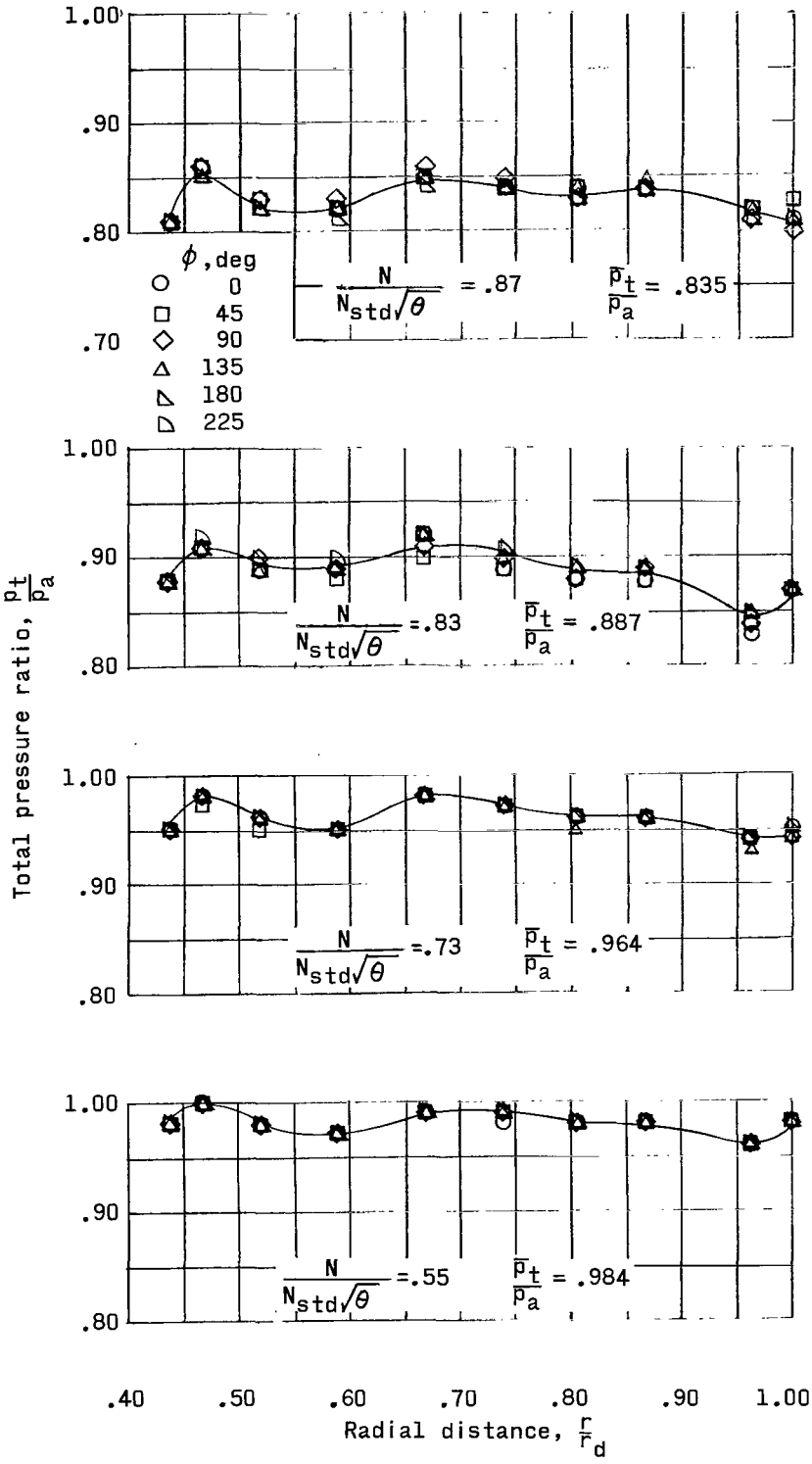

Figure 14.- Effect of corrected engine speed on flow distribution with auxiliary doors closed. $\Delta x = 0$.

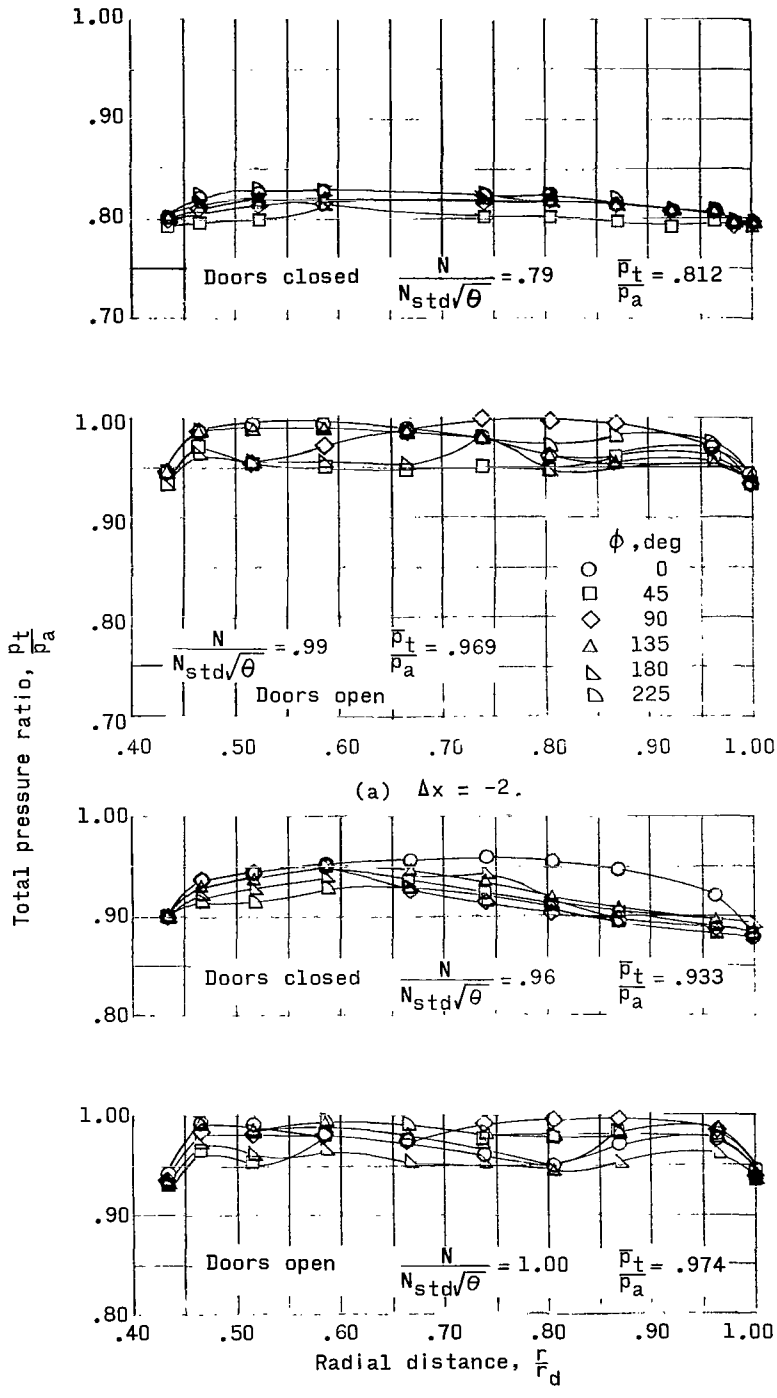

Figure 15.- Effect of centerbody position on flow distribution with auxiliary doors open and closed.

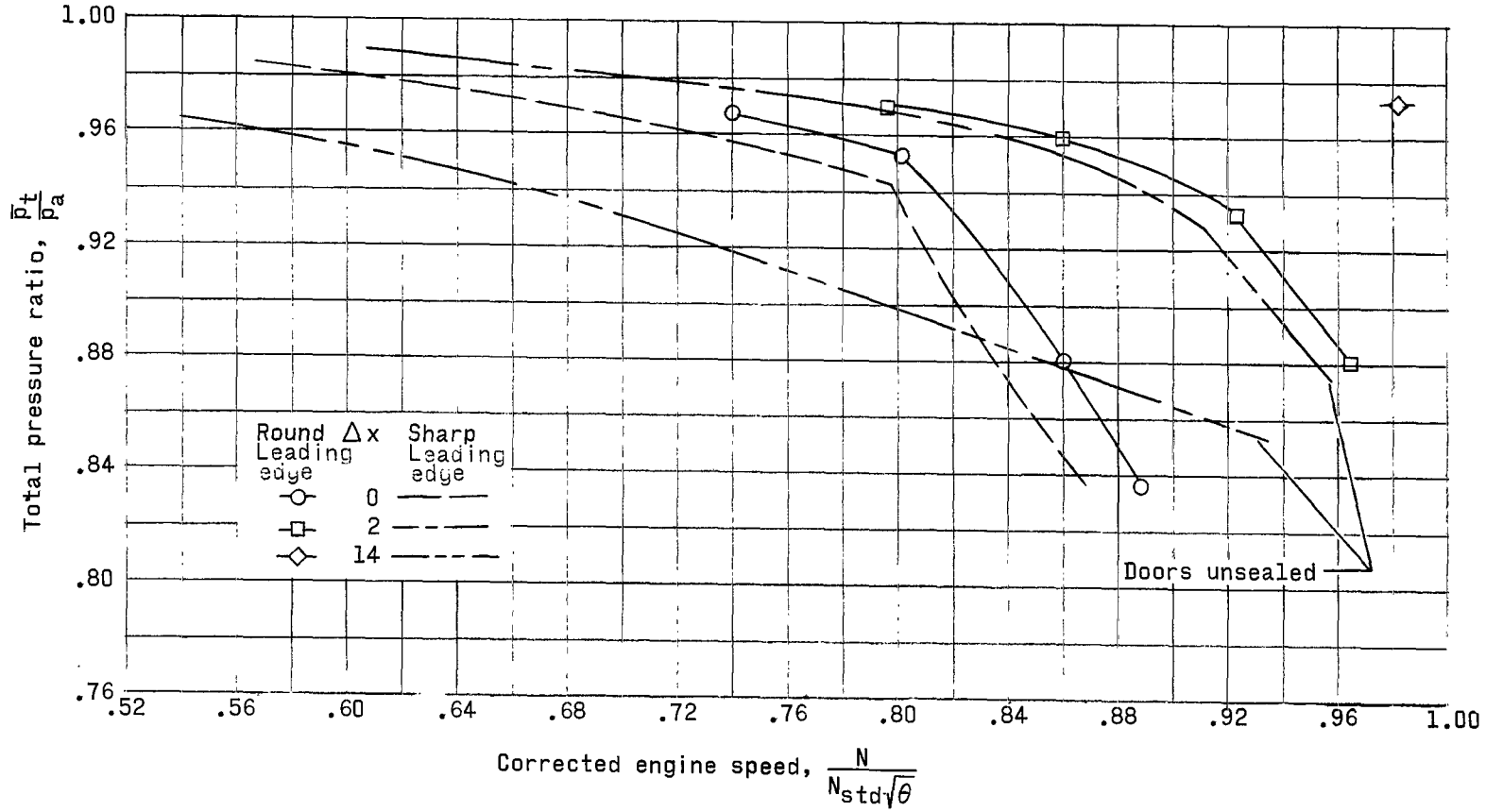

Figure 16.- Effect of leading-edge shape on inlet total-pressure ratio. Flagged symbols indicate doors sealed.

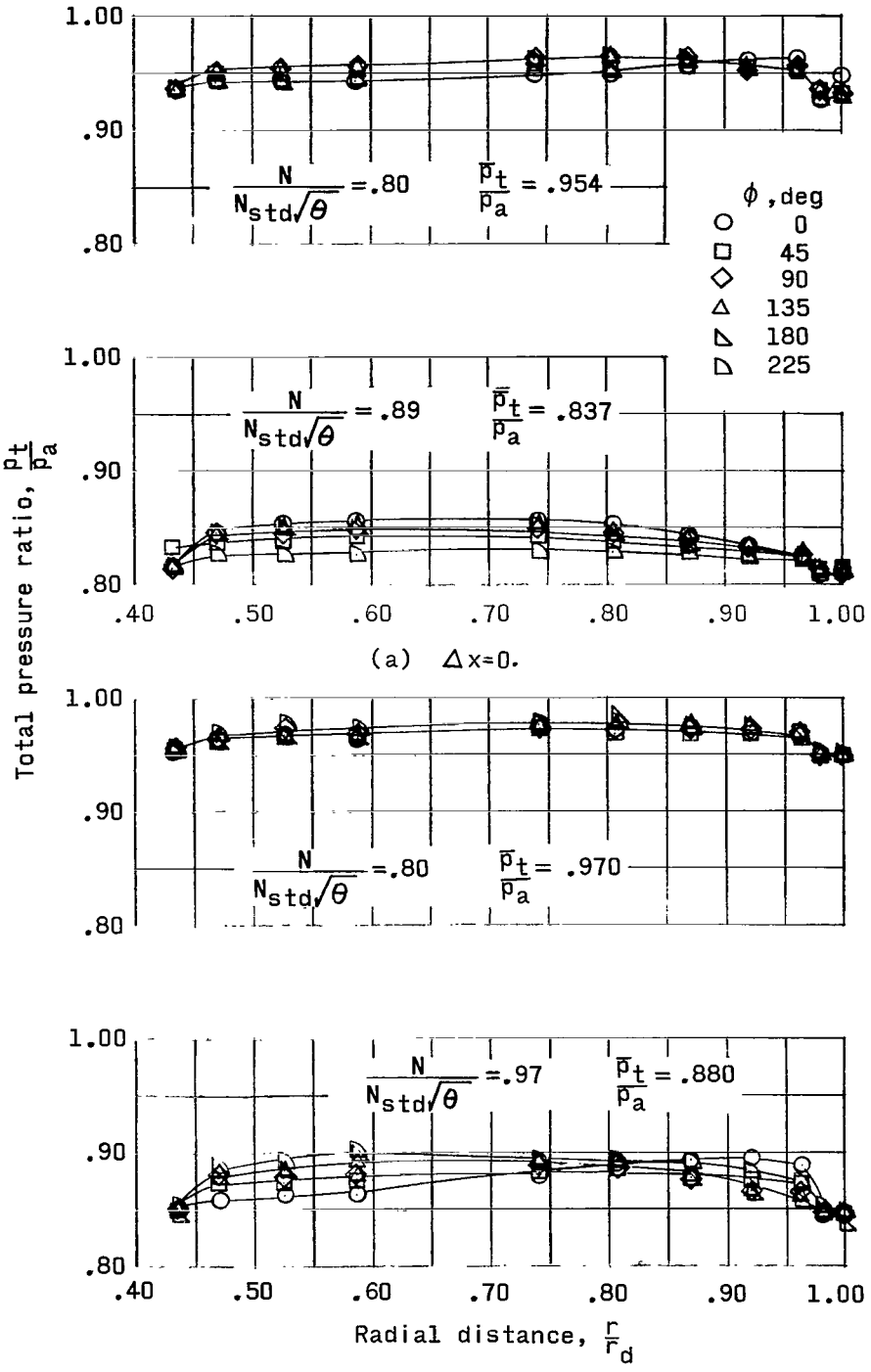

Figure 17.- Flow distribution for rounded leading-edge shape.

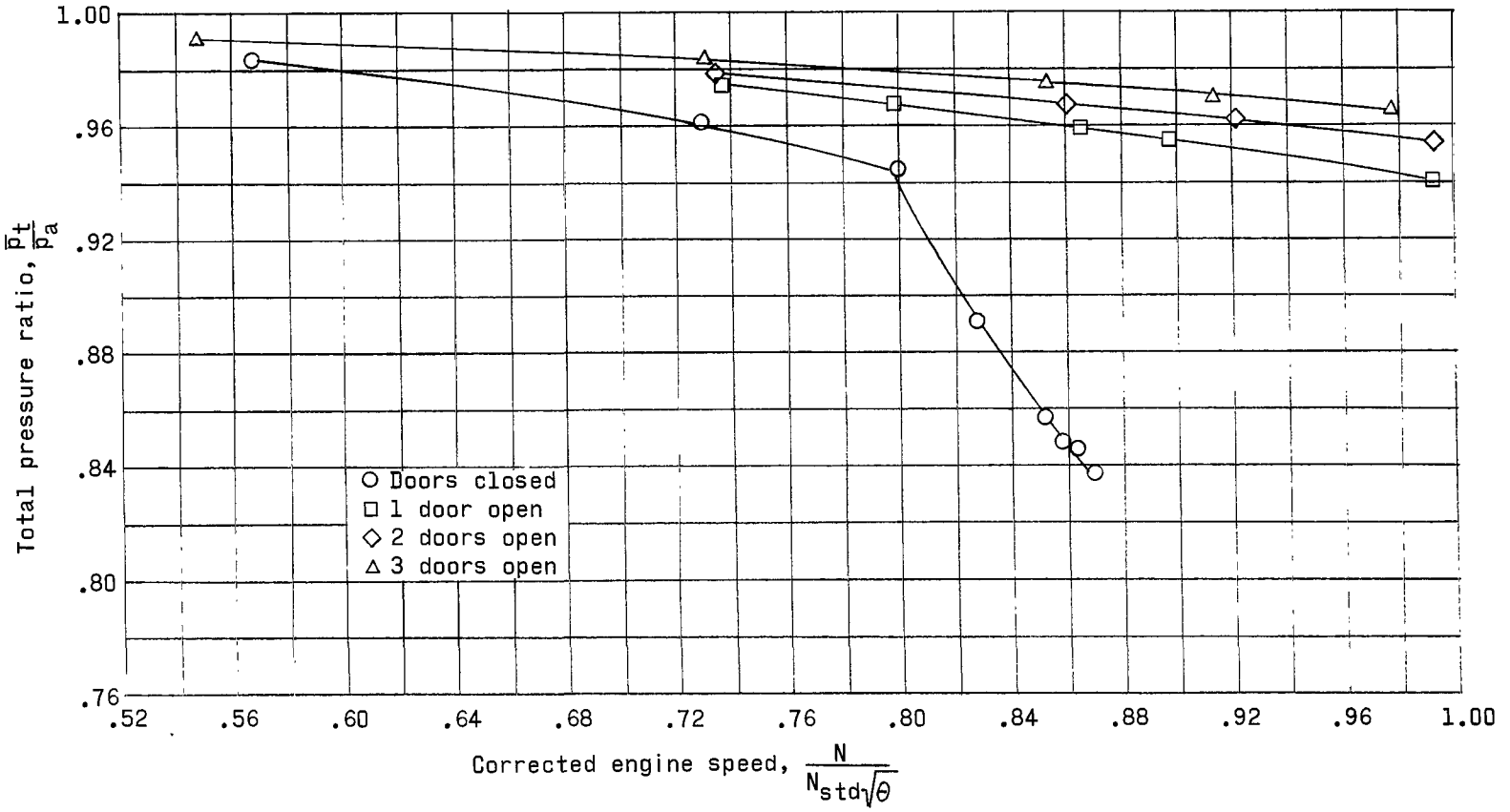

Figure 18.- Effect of opening one or two auxiliary doors on inlet total-pressure ratio. $\Delta x = 0$.

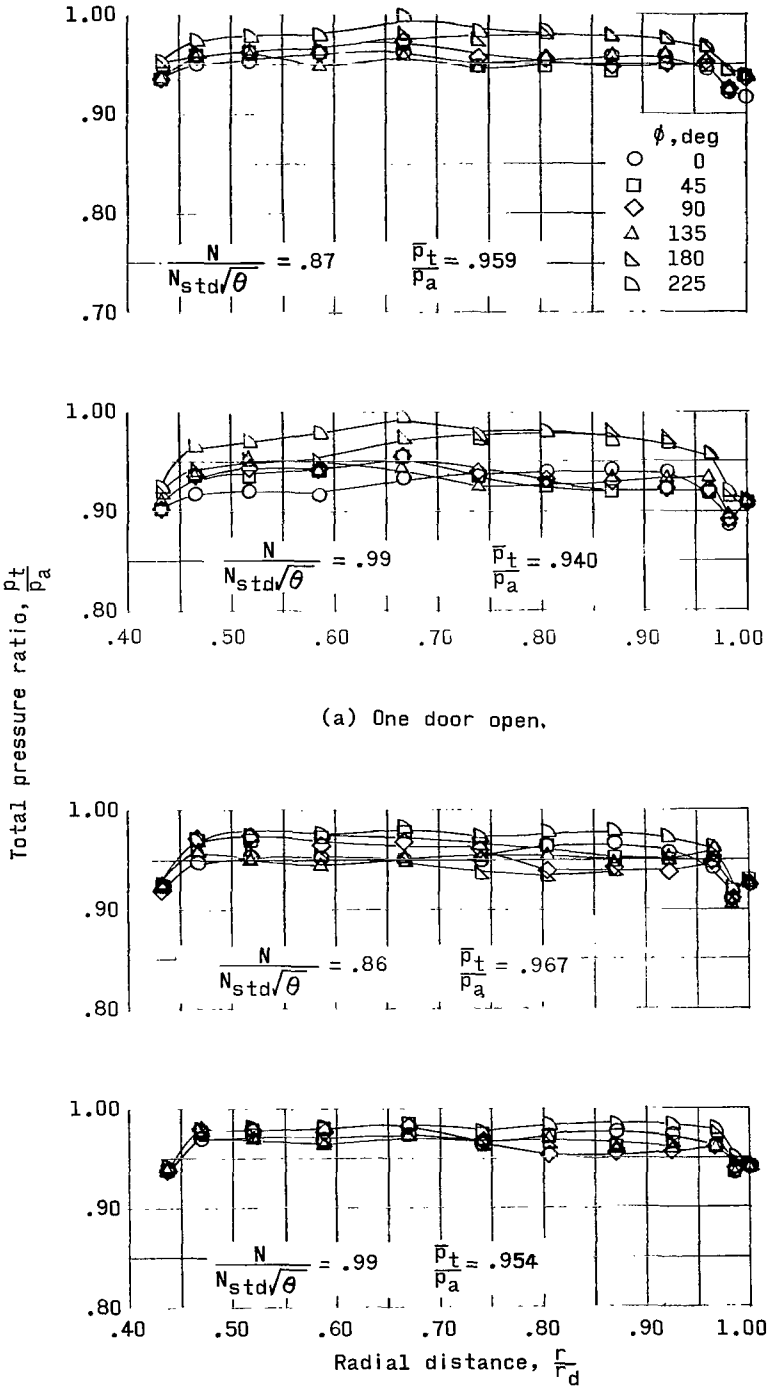

Figure 19.- Effect of opening one or two auxiliary doors on flow distribution. $\Delta x = 0$.

Curve	Condition	$\frac{N}{N_{std}\sqrt{\theta}}$	Speed, rpm	Δx
———	Choked	84.7	11,780	0
– – – – –	Unchoked	84.7	11,780	14

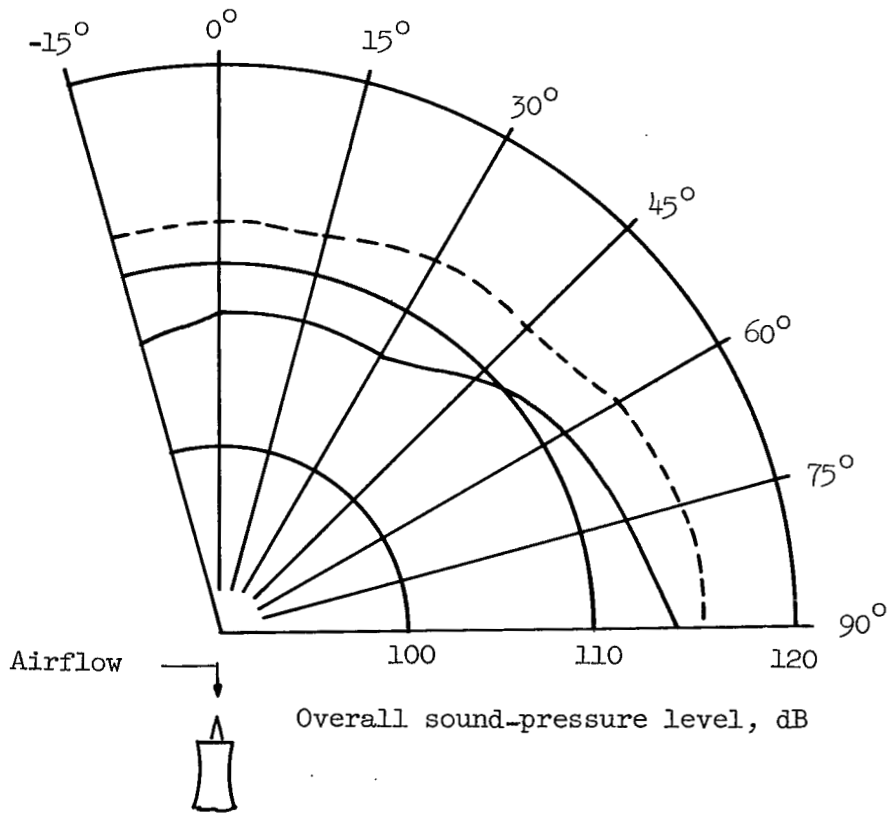

Figure 20.- Overall noise radiation patterns measured on a 25-foot radius for choked and unchoked inlet flow conditions. Data are for turbojet engine at constant speed and for two different inlet centerbody positions.

Curve	Condition	$\frac{N}{N_{std}\sqrt{\theta}}$	Speed, rpm	Δx
———	Choked	70.3	9640	-2
- - - - -	Unchoked	67.4	9240	-2

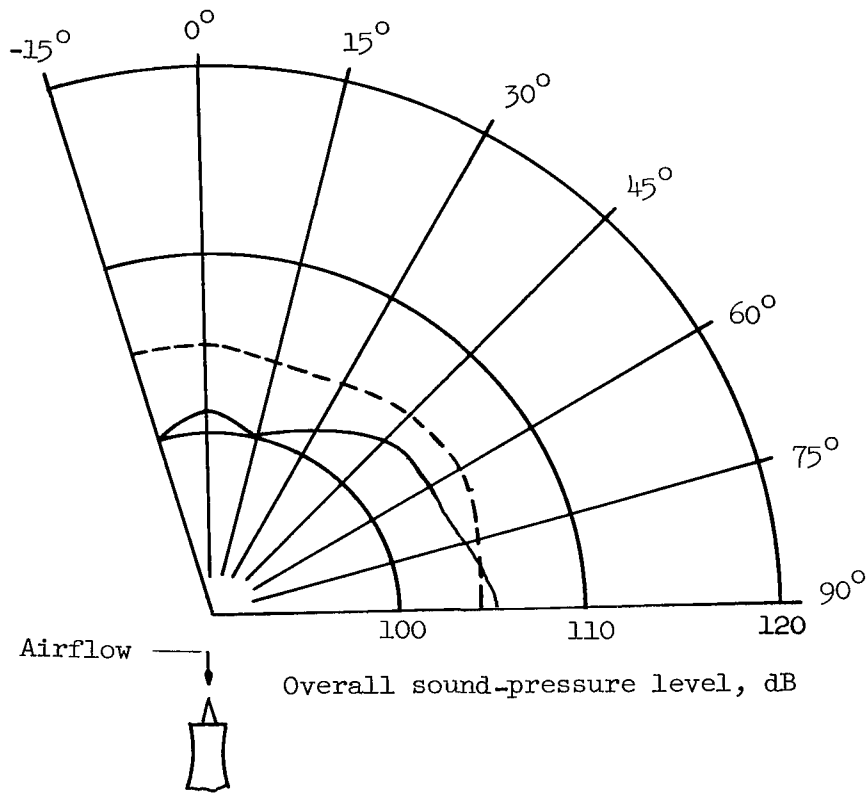

Figure 21.- Overall noise radiation patterns measured on a 25-foot radius for choked and unchoked inlet flow conditions. Data are for turbojet engine at constant inlet centerbody position and for two different speeds.

Curve	Condition	$\frac{N}{N_{std}\sqrt{\theta}}$	Speed, rpm	Δx
———	Choked	84.7	11,780	0
- - - - -	Unchoked	84.7	11,780	14

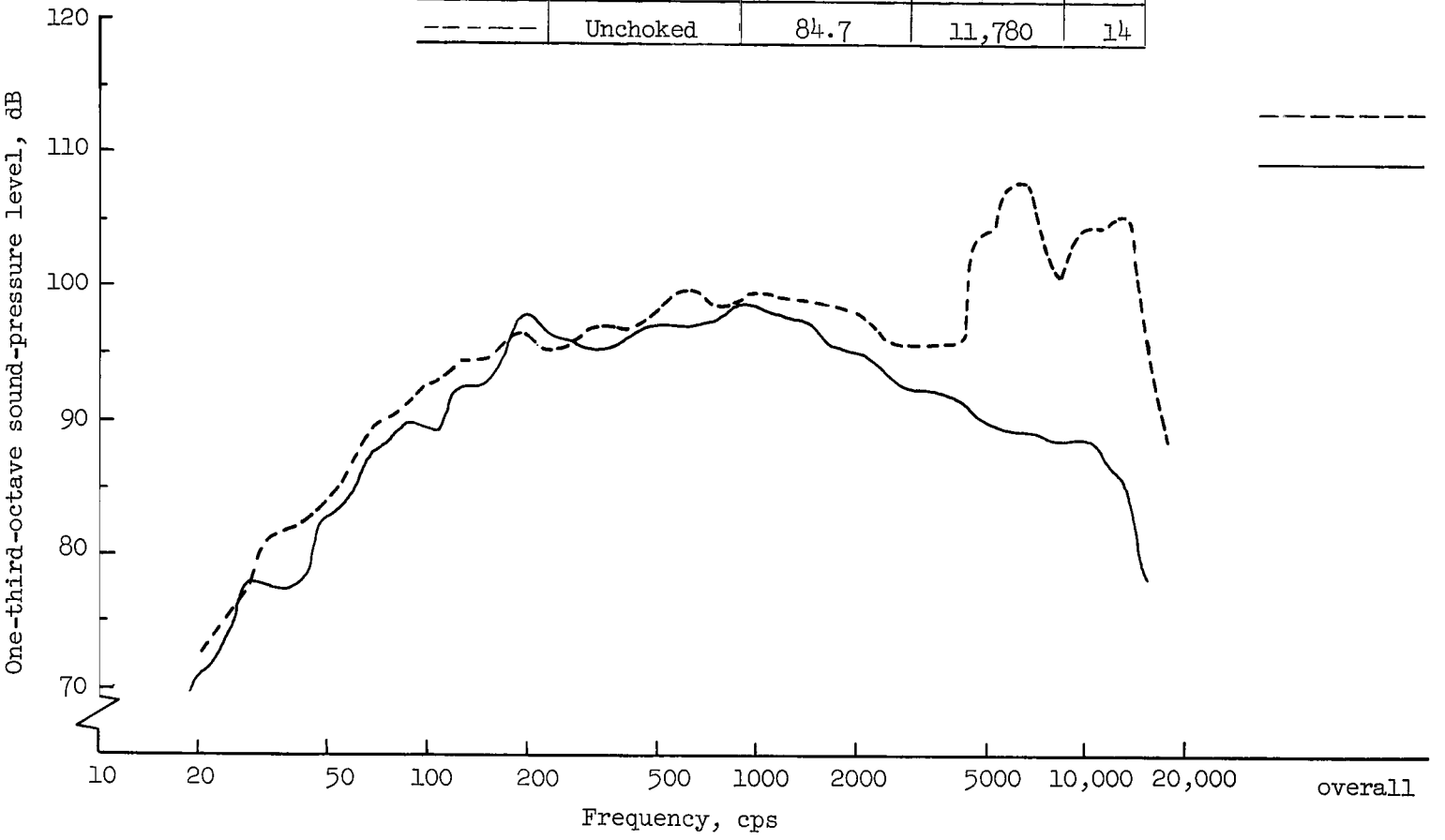

Figure 22.- One-third-octave band noise spectra measured on a 25-foot radius at the 30° azimuth position for choked and unchoked inlet flow conditions. Data are for turbojet engine at constant speed and for two different inlet centerbody positions.

Curve	Condition	$\frac{N}{N_{std}\sqrt{\theta}}$	Speed, rpm	Δx
———	Choked	70.3	9640	-2
- - - -	Unchoked	67.4	9240	-2

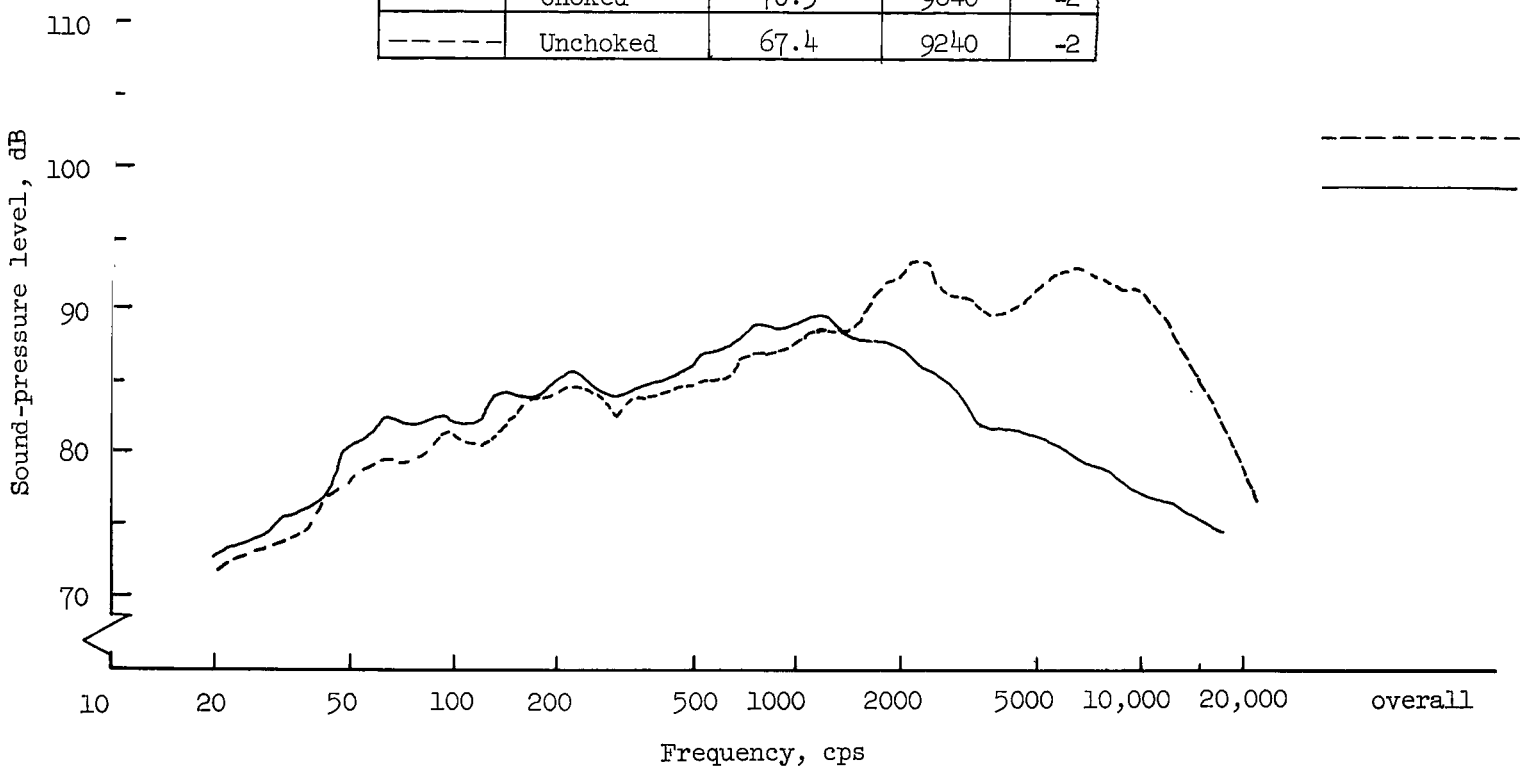

Figure 23.- One-third-octave band noise spectra measured on a 25-foot radius at the 30° azimuth position for choked and unchoked inlet flow conditions. Data are for turbojet engine at constant inlet centerbody position and for two different speeds.

Curve	Condition	$\frac{N}{N_{std}\sqrt{\theta}}$	Speed, rpm	Δx
———	Choked	84.7	11,780	0
– – – –	Unchoked	84.7	11,780	14

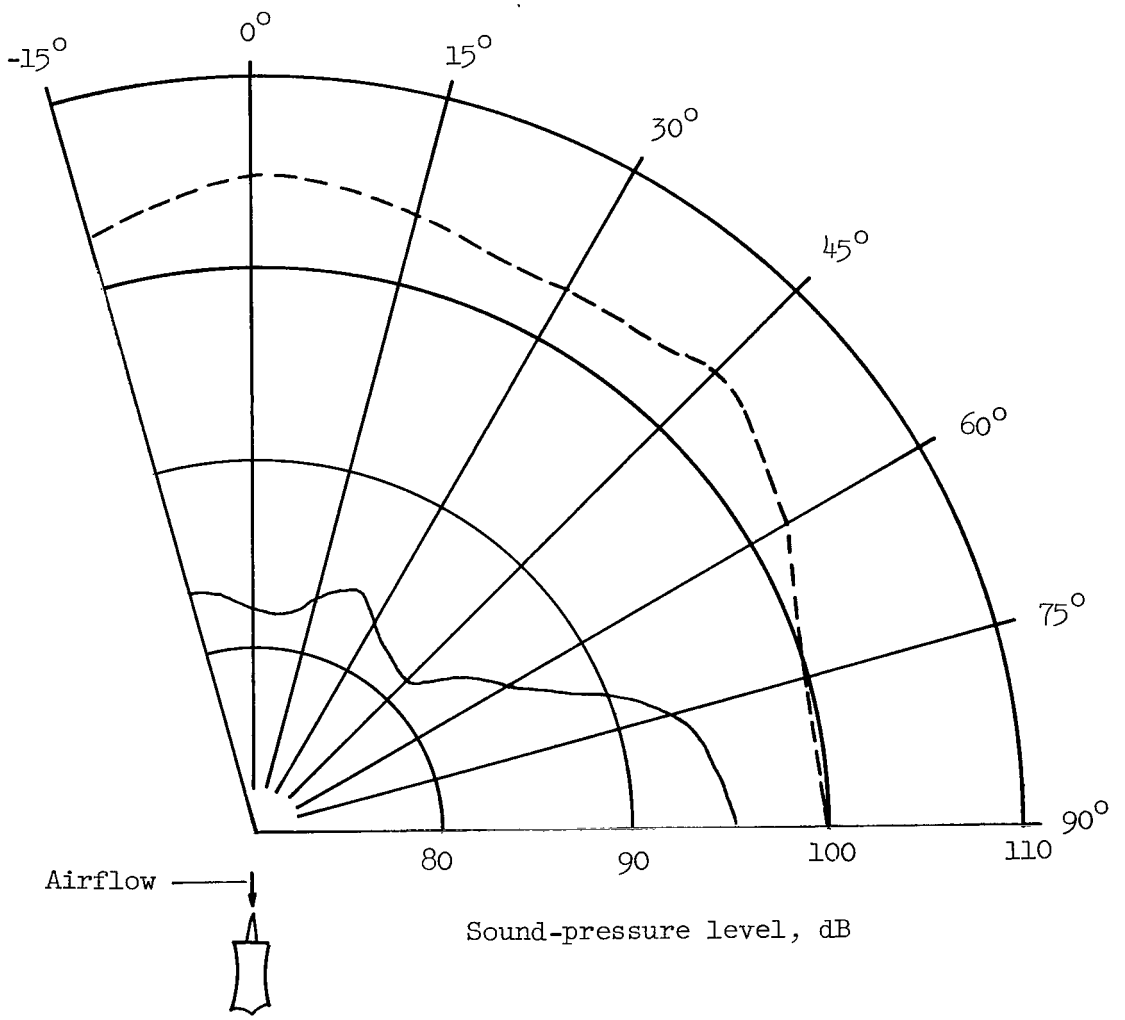

Figure 24.- Narrow-band (50 cps) radiation patterns of sound-pressure level at the fundamental blade-passage frequency measured on a 25-foot radius for choked and unchoked inlet flow conditions. Data are for turbojet engine at constant speed and for two different inlet centerbody positions.

Curve	Condition	$\frac{N}{N_{std}\sqrt{\theta}}$	Speed, rpm	Δx
———	Choked	70.3	9640	-2
- - - - -	Unchoked	67.4	9240	-2

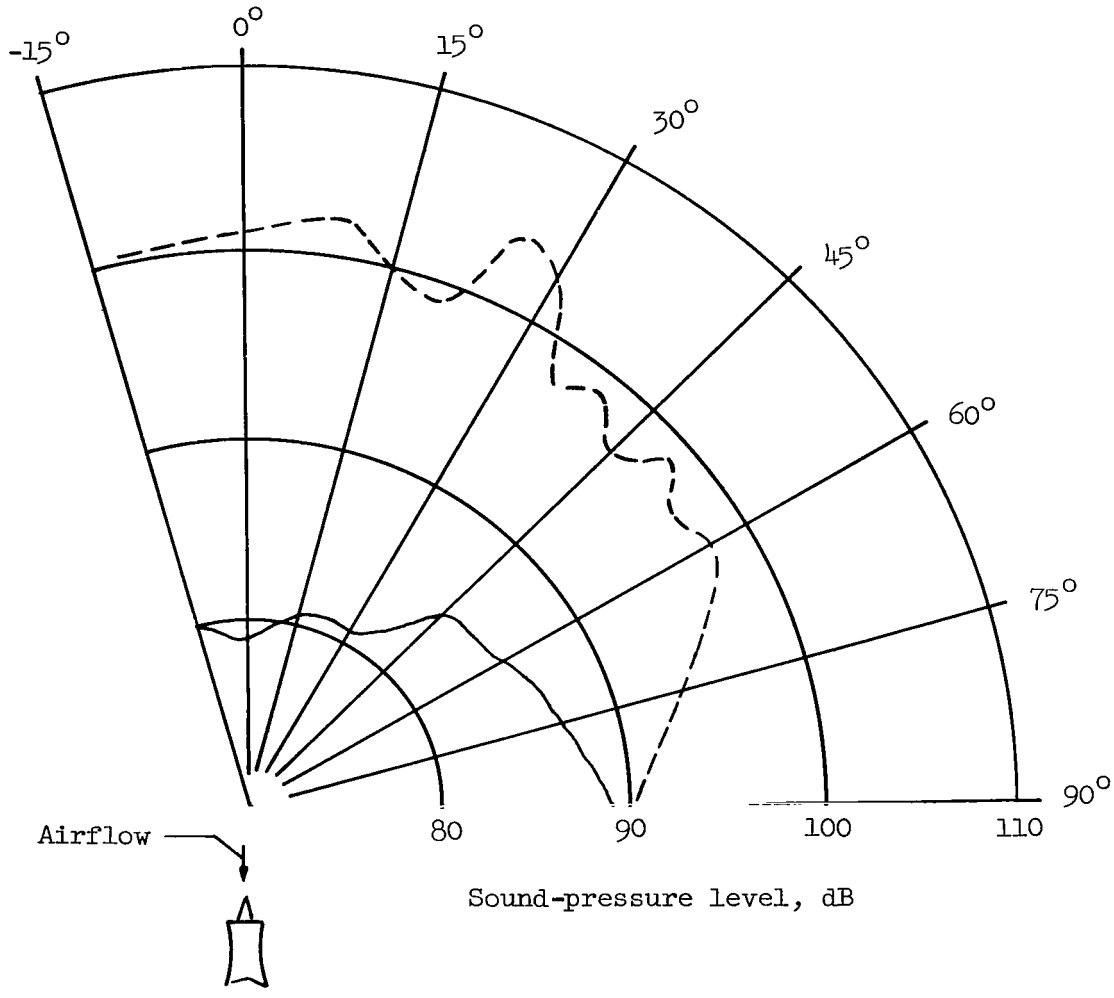

Figure 25.- Narrow-band (50 cps) radiation patterns of sound-pressure level at the fundmental blade-passage frequency measured on a 25-foot radius for choked and unchoked inlet flow conditions. Data are for turbojet engine at constant inlet centerbody position and for two different speeds.

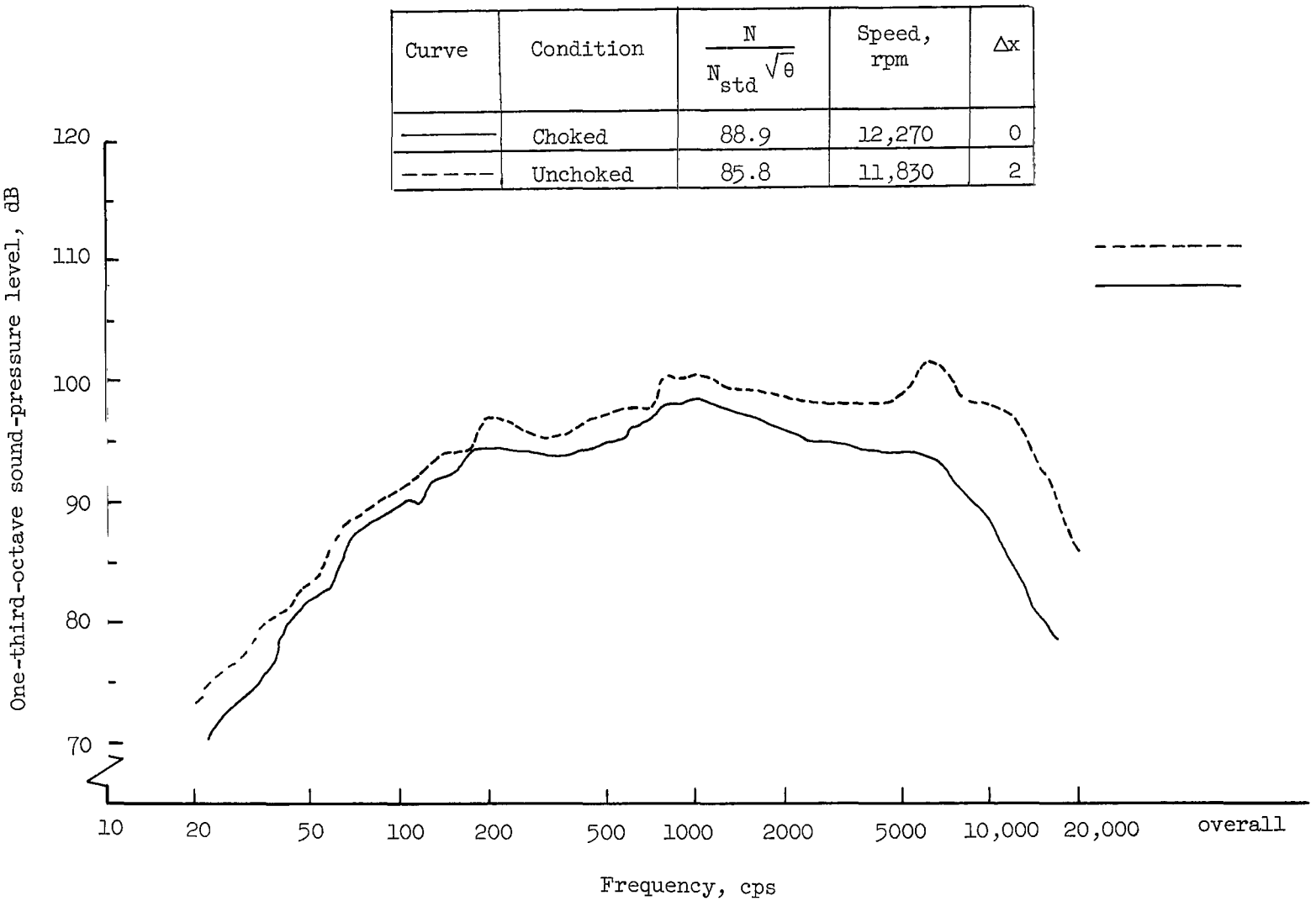

Figure 26.- One-third-octave band noise spectra measured on a 25-foot radius at the 30° azimuth position for choked and unchoked inlet flow conditions. Data are for turbojet engine at nearly constant thrust and for two different speeds and inlet centerbody positions.

Curve	Condition	$\frac{N}{N_{std}\sqrt{\theta}}$	Speed, rpm	Δx
———	Choked	70.3	9640	-2
– – – –	Unchoked	67.4	9240	-2

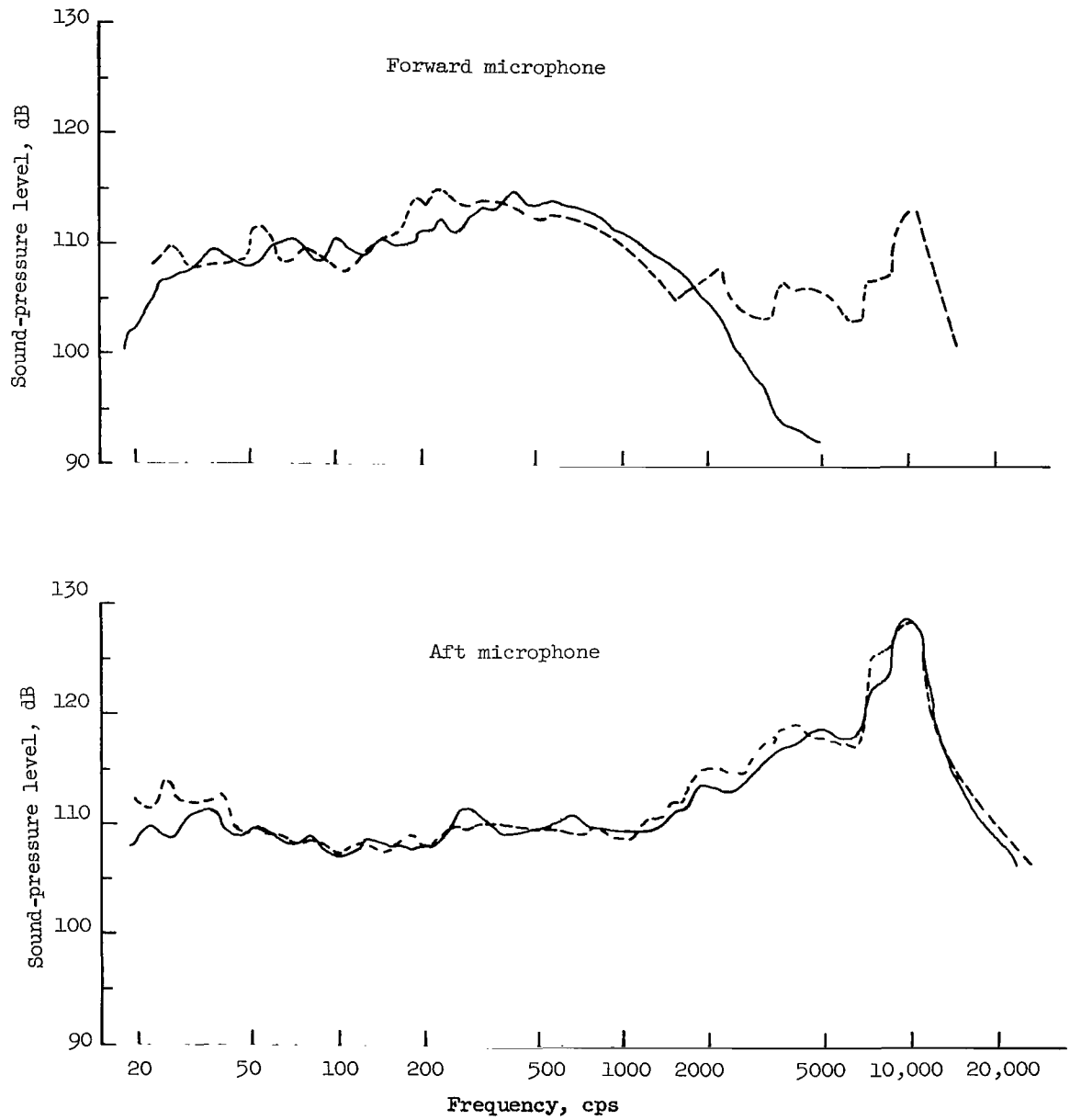

Figure 27.- One-third-octave band noise spectra measured inside the inlet for choked and unchoked inlet flow conditions. Data are for turbojet engine at constant inlet centerbody position and for two different speeds.

"The aeronautical and space activities of the United States shall be conducted so as to contribute . . . to the expansion of human knowledge of phenomena in the atmosphere and space. The Administration shall provide for the widest practicable and appropriate dissemination of information concerning its activities and the results thereof."

—NATIONAL AERONAUTICS AND SPACE ACT OF 1958

NASA SCIENTIFIC AND TECHNICAL PUBLICATIONS

TECHNICAL REPORTS: Scientific and technical information considered important, complete, and a lasting contribution to existing knowledge.

TECHNICAL NOTES: Information less broad in scope but nevertheless of importance as a contribution to existing knowledge.

TECHNICAL MEMORANDUMS: Information receiving limited distribution because of preliminary data, security classification, or other reasons.

CONTRACTOR REPORTS: Scientific and technical information generated under a NASA contract or grant and considered an important contribution to existing knowledge.

TECHNICAL TRANSLATIONS: Information published in a foreign language considered to merit NASA distribution in English.

SPECIAL PUBLICATIONS: Information derived from or of value to NASA activities. Publications include conference proceedings, monographs, data compilations, handbooks, sourcebooks, and special bibliographies.

TECHNOLOGY UTILIZATION PUBLICATIONS: Information on technology used by NASA that may be of particular interest in commercial and other non-aerospace applications. Publications include Tech Briefs, Technology Utilization Reports and Notes, and Technology Surveys.

Details on the availability of these publications may be obtained from:

SCIENTIFIC AND TECHNICAL INFORMATION DIVISION

NATIONAL AERONAUTICS AND SPACE ADMINISTRATION

Washington, D.C. 20546